Cascaded forward Brillouin scattering to all Stokes orders

2017 New J. Phys. 19 023021

(http://iopscience.iop.org/1367-2630/19/2/023021)

New Journal of Physics
The open access journal at the forefront of physics

Deutsche Physikalische Gesellschaft DPG
IOP Institute of Physics

Published in partnership with: Deutsche Physikalische Gesellschaft and the Institute of Physics

OPEN ACCESS

RECEIVED
8 September 2016

REVISED
13 December 2016

ACCEPTED FOR PUBLICATION
16 January 2017

PUBLISHED
9 February 2017

PAPER

Cascaded forward Brillouin scattering to all Stokes orders

C Wolff[1,2], B Stiller[1,3], B J Eggleton[1,3], M J Steel[1,4] and C G Poulton[1,2]

[1] Centre for Ultrahigh bandwidth Devices for Optical Systems (CUDOS), Australia
[2] School of Mathematical and Physical Sciences, University of Technology Sydney, NSW 2007, Australia
[3] Institute of Photonics and Optical Science (IPOS), School of Physics, University of Sydney, NSW 2006, Australia
[4] MQ Photonics Research Centre, Department of Physics and Astronomy, Macquarie University Sydney, NSW 2109, Australia

E-mail: christian.wolff@uts.edu.au

Keywords: stimulated Brillouin scattering, opto-mechanics, nano-photonics

Abstract

Inelastic scattering processes such as Brillouin scattering can often function in cascaded regimes and this is likely to occur in certain integrated opto-acoustic devices. We develop a Hamiltonian formalism for cascaded Brillouin scattering valid for both quantum and classical regimes. By regarding Brillouin scattering as the interaction of a single acoustic envelope and a single optical envelope that covers all Stokes and anti-Stokes orders, we obtain a compact model that is well suited for numerical implementation, extension to include other optical nonlinearities or short pulses, and application in the quantum-optics domain. We then theoretically analyze *intra-mode* forward Brillouin scattering (FBS) for arbitrary waveguides with and without optical dispersion. In the absence of optical dispersion, we find an exact analytical solution. With a perturbative approach, we furthermore solve the case of weak optical dispersion. Our work leads to several key results on intra-mode FBS. For negligible dispersion, we show that cascaded intra-mode FBS results in a pure phase modulation and discuss how this necessitates specific experimental methods for the observation of fiber-based and integrated FBS. Further, we discuss how the descriptions that have been established in these two classes of waveguides connect to each other and to the broader context of cavity opto-mechanics and Raman scattering. Finally, we draw an unexpected striking similarity between FBS and discrete diffraction phenomena in waveguide arrays, which makes FBS an interesting candidate for future research in quantum-optics.

1. Introduction

The phenomenon of Brillouin scattering, whereby an acoustic field mediates transitions between optical modes in an optical waveguide [1–3], has been the focus of intense research interest in recent years, driven by a suite of key applications in nanophotonics ranging from microwave photonic filters to novel light sources [4]. Brillouin scattering can be categorized according to the direction of light scattered by the phonon field: *backward* Brillouin scattering, by broad consensus called stimulated Brillouin scattering (SBS) because of the self-reinforcing nature of the phenomenon, arises commonly in optical fibers and results from the interaction of optical guided waves with a longitudinal acoustic wave with a wave length of only few hundred nanometers. In contrast, *forward* Brillouin scattering (FBS) arises due to the interaction of light with long-wavelength acoustic modes. Depending on whether the interaction occurs within the same optical mode (intra-mode FBS) or between different optical modes (inter-mode FBS), the relevant acoustic field either forms a transverse wave with wave length on the order of centimeters or complex a torsional or flexural mode with intermediate wave length (see figure 1). Although observed experimentally as early as 1985 [5] in conventional step index fibers, FBS appears most naturally in waveguides that possess complex transverse structure; FBS has been observed in photonic crystal fibers (PCFs) and tapers [6–12], while the parallel development of on-chip integrated optical circuits has led to experimental observation of FBS in semiconductor nanowires [13, 14], and theoretical consideration of slot waveguides [15] and hybrid photonic-phononic waveguides [16]. The observation that FBS is much easier to generate in

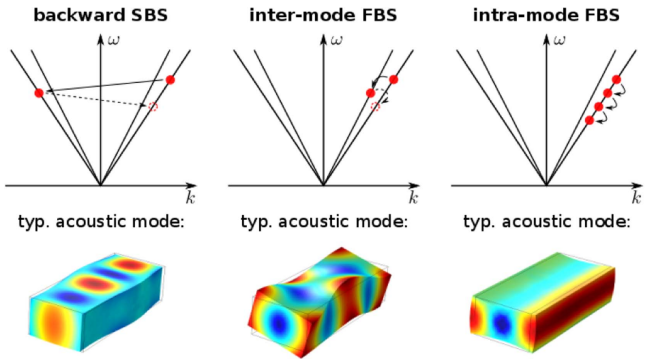

Figure 1. Sketch of the three main variants of guided Brillouin scattering: backward (stimulated) scattering (left), inter-mode forward scattering (center) and intra-mode forward scattering (right). For each case the figure schematically shows the acoustically mediated transitions within the optical dispersion relation as well as typical examples for the corresponding acoustic modes. Note that only for intra-mode forward scattering (right panel) all Stokes order are connected by the same acoustic mode (i.e. same symmetry, wave number and frequency). This motivates why intra-mode FBS is particularly prone to cascading.

integrated silicon circuits than its backward counterpart [14, 17, 18] means that FBS is critically important for applications that seek to harness the interaction of sound and light on the nanoscale.

The established theory for Brillouin processes, in which a single pair of optical fields are related by an acoustic mode, has been developed from the study of backward SBS [2, 19, 20], backward GAWBS [21] and cladding BS [22] in homogeneous materials and optical fibers. With some important modifications [18, 23, 24], for backward SBS this formalism can be directly applied to the nanostructures that are of recent interest. However the existing theory is not well-suited to the study of FBS. The main reason for this is the phenomenon of cascading, whereby the generation of a single, or first-order, Stokes line results in multiple follow-on orders. Under certain conditions cascading can occur in backwards SBS, however the process usually only arises in the presence of reflections or resonances [25, 26]. By contrast, cascading arises in FBS because of the less-stringent phase-matching requirements. In principle the existence of large numbers of Stokes lines in FBS could be addressed by an ad hoc expansion of the existing formalism, however this approach restricts the optical spectrum to a comb of Stokes lines, introduces artifacts if the expansion of Stokes orders is truncated, and becomes rather cumbersome in the presence of optical dispersion or in combination with other optical nonlinearities such as Raman scattering or the instantaneous Kerr effect. This approach also requires severe restrictions on the optical fields, which must vary slowly on the time and length scales of the *acoustic* field, and on the opto-acoustic response, which is assumed to be perfectly Lorentzian. The range of experimental situations that can be treated with existing approaches is therefore highly limited. With the recent intense interest in the generation of FBS in nanostructures, a general theory that fully describes FBS is not only essential to gain physical insight and to guide experiments, but will form part of the ongoing program aiming to adapt Brillouin processes for use in nanophotonics and to unify the theory with that of traditional optomechanics [27].

Here we present a new and rigorous formulation of FBS that includes cascading to all orders. To this end, we allow optical envelopes to cover any number of (anti-)Stokes lines, which reduces fully cascaded FBS to an interaction between one optical and one mechanical envelope. Figure 2 shows a schematic of a prototypical system: a modulated pump is injected into a waveguide that supports nearly transversal mechanical eigenmodes. The pump modulation can be either a dedicated Stokes seed as commonly used in silicon photonics experiments or the inevitable intensity noise of the pump laser. For vanishing dispersion, our model has a full general analytical solution in the sense that the optical field at the waveguide's output is given as an explicit integral of the arbitrary input envelope. A key finding is that without dispersion the optically driven vibrations only cause an additional optical phase modulation. This is in agreement with the recent theoretical observation that FBS in the absence of dispersion has negative single-pass gain [18]. We then show that weak dispersion leads to two different regimes: in one regime dispersion washes out intensity fluctuations of an incident pump laser while generating additional phase noise. In the other regime, it leads to self-amplifying dynamics along the waveguide. We also demonstrate the great similarity of FBS with Raman scattering as it is encountered, for example, in the context of soliton dynamics. Finally, we find an unexpected striking similarity between dispersionless FBS and discrete diffraction in waveguide arrays. This makes optically driven FBS an interesting candidate for few-photon experiments. Our single-envelope formulation of cascaded FBS is ideally suited for this type of problem, as it conveniently describes superpositions of different Stokes orders with a single operator.

Our formalism allows arbitrary optical spectra spanning several Stokes shifts, including soliton-like pulses and it facilitates the inclusion of optical dispersion and other optical nonlinearities, which we demonstrate for

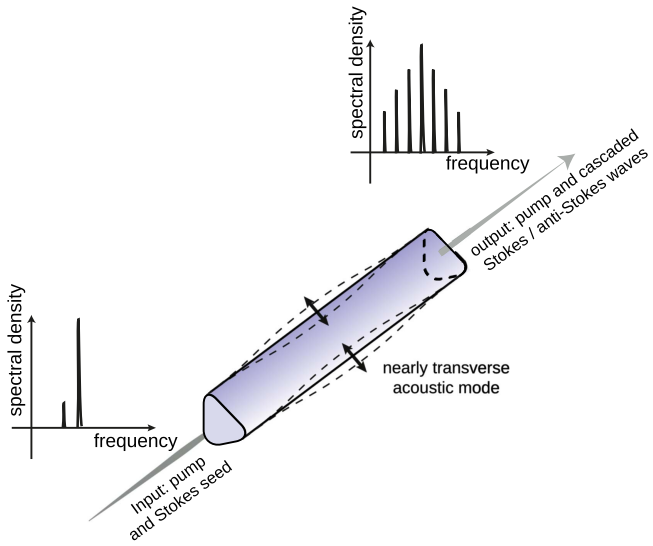

Figure 2. Schematic of a prototypical setup for cascaded forward Brillouin scattering: in a waveguide (e.g. a nanowire, rib waveguide or an optical fiber) a mechanical vibration with near-zero wave number and group velocity is excited by an incident optical pump and a weak Stokes seed (e.g. due to intensity noise in the pump laser). This results in the exiting light being predominantly phase-modulated with pronounced higher-order (anti-)Stokes side bands.

Raman-scattering and the Kerr effect. Furthermore, our formalism illuminates the placement of FBS within the family of optical nonlinearities. FBS bears resemblance with several other scattering phenomena, and exhibits different characteristics that depend on the parameters of the experiment. This chimeric quality is reflected in the different names FBS has been given, each of which highlights specific aspects of the phenomenon. The term 'guided acoustic wave Brillouin scattering' (GAWBS) [5, 6, 8, 10, 11] emphasizes the confined nature of the acoustic wave and the directionality of FBS in silica fibers. In contrast, 'Raman-like light scattering' [7, 28] highlights that (unlike in backward SBS) the Stokes shift is nearly independent of the optical wavelength and that FBS easily leads, as in the Raman process, to cascading. Finally, 'forward stimulated Brillouin scattering' (FSBS) [16, 23] draws the strong formal connection with backward (stimulated) Brillouin scattering.

A result of the formalism presented here is that these aspects are unified: specific observations can be explained with the fact that fibers and integrated waveguides can be quite different in optical loss, dispersion, power handing, length, and opto-mechanical interaction strength. For this reason we have adopted the very general term 'FBS' and devote section 6.2 in our discussion to the different regimes referred to by the above mentioned terms and the corresponding measurement techniques.

This paper consists of two main blocks: first we derive our theoretical model for cascaded FBS from first principles and show its consistency with established theory. Starting in section 4, we proceed to analyze the model. Each of these two blocks is fairly self-contained; in particular, we re-state the basic equations of our model at the beginning of section 4. Readers who are mostly interested in the results and their discussion can skip section 3 on a first reading. The structure of this paper is as follows: in section 2, we state the approximations and assumptions that are required for describing an optical pump and all (anti-)Stokes orders in an optical band with a single envelope function. We also comment on the differences between a classical and a quantum-mechanical description. In section 3, we then go on to first derive the quantum-mechanical Hamiltonian for Brillouin scattering in a single-envelope picture and state both quantum-mechanical and classical equations of motion, which we then specialize for intra-mode forward scattering. We demonstrate how the established multi-envelope theory is derived from this. Next, we solve the dispersionless case analytically for any optical input in section 4. Based on this result, the case of weak optical dispersion and shallow optical intensity variations is solved perturbatively in section 5. Section 6 finally concludes our paper with an in-depth discussion and a summary of the main findings.

2. Approximations, assumptions and theoretical approach for cascaded Brillouin scattering

The established coupled mode theory [2, 19, 20, 23, 24, 29] of SBS is centered around two approximations: a restrictive slowly varying envelope approximation (SVEA) for the wave propagation and a restrictive rotating wave approximation (RWA) for the opto-acoustic interaction. The approximations are restrictive in the sense

that all but the most slowly varying interaction terms are neglected and that the acoustic envelopes as well as the envelopes describing individual Stokes orders (usually only the pump and the first Stokes band) only vary on a time scale larger than the acoustic period. In intra-mode FBS settings the acoustic field is assumed to be the same for the interaction between each pair of adjacent optical lines.

This approach has two main disadvantages for the study of problems where cascading effects are relevant. Firstly, each Stokes order requires an additional differential equation, which can become cumbersome if other nonlinear effects such as Kerr-induced four-wave mixing and optical dispersion are to be included. This is mostly a technical problem. Secondly, the decomposition into individual Stokes orders requires a very restrictive implementation of the SVEA and the RWA in that the optical envelopes have to vary slowly on the order of the *acoustic* time and length scales. In the same vein, the opto-acoustic interaction term is stripped of all contributions that deviate from a perfect Lorentzian response. This restriction of the established theory precludes for example the description of opto-acoustic dynamics of light pulses that vary on the acoustic time scale. We therefore seek a less restrictive description of Brillouin scattering.

An optical envelope can cover several THz and still be considered slowly varying, thus one single optical envelope is sufficient to describe all Stokes orders at once. However, this is in conflict with the RWA as it is commonly applied to the opto-acoustic interaction term: in the established literature, the interaction term is averaged over a time window much longer than the acoustic period. Instead, we have to relax the RWA to allow for variations on the same time scale as the optical envelope, i.e. several multiples of the acoustic period. As a result, such a model has to allow for far off-resonant excitations of the mechanical system and for example include static deformations. Consequently, the acoustic amplitude cannot be described as a slowly varying envelope, but instead has to explicitly contain the time dependence of the mechanical oscillations. We note that the single-envelope picture outlined above is quite common in short-pulse Raman physics [2, 3, 30]. Furthermore, we remark that a formulation of non-cascaded backward Brillouin scattering based on a non-slowly varying envelope picture has been studied in the past [31].

Brillouin scattering can be formulated as a problem of classical physics e.g. based on a Lagrangian or a coupled mode picture, both of which allow for an elegant incorporation of loss. Alternatively, if can be described based on a classical or quantum-mechanical Hamiltonian, which we feel have the advantage that the different forms of RWA can be presented more clearly compared to the two non-Hamiltonian approaches. We therefore choose to derive our single-envelope description from first principles via a Hamiltonian formalism. As it turns out, there is basically no difference in complexity between a classical and quantum formulation Hamiltonian: the quantum description only adds a few factors of $\sqrt{\hbar\omega}$ in the equations (1)–(27), the use of commutators instead of Poisson brackets and the intermediate result equations (26) and (27). This presents the opportunity to lay the formal foundation for later work on quantum-optics using FBS as a bonus to our analysis of cascaded classical FBS. We therefore derive the framework in a quantum-mechanical Hamiltonian picture and switch to the classical picture at the end of section 3, where we also add the loss terms that are well known from the literature. During revisions of this manuscript, a study on quantum Brillouin scattering based on a related relaxed RWA appeared online [32].

3. Hamiltonian and equations of motion

We follow the example of [29] and start our investigation with the opto-acoustic Hamiltonian. From this, we derive equations of motion for the quantum mechanical amplitudes of the optical and acoustic fields. Originating from a Hamiltonian representation without external baths, this model is lossless. We then move on to the classical realm, where we also introduce acoustic loss. This is adequate to describe most experiments.

The Hamiltonian for opto-acoustic interactions in a longitudinally invariant waveguide (oriented along z) can be expressed in a modal expansion of the form [29]

$$\mathcal{H} = \sum_{\alpha}\int_{-\infty}^{\infty} \mathrm{d}k\ \hbar\omega_{\alpha k}\hat{a}_{\alpha k}^{\dagger}\hat{a}_{\alpha k} + \sum_{\beta}\int_{-\infty}^{\infty} \mathrm{d}q\ \hbar\Omega_{\beta q}\hat{b}_{\beta q}^{\dagger}\hat{b}_{\beta q} + \mathcal{V}, \tag{1}$$

where $\mathcal{V}$ is the opto-acoustic interaction term, $\hat{a}_{\alpha k}$ is the annihilation operator for a photon in the αth optical mode with wave number k and energy $\hbar\omega_{\alpha k}$, and $\hat{b}_{\beta q}$ likewise for a phonon in the βth acoustic mode with wave number q and energy $\hbar\Omega_{\beta q}$. The ladder operators $\hat{a}_{\alpha k}$ and $\hat{b}_{\beta q}$ are not to be confused with the classical envelope functions $a_{\alpha}(z,\ t)$ and $b_{\beta}(z,\ t)$ that will be introduced towards the end of this section. We furthermore introduce the electric induction field operator and the mechanical strain operator

$$\hat{\mathbf{D}} = \sum_{\alpha} \frac{1}{2\sqrt{\pi}} \int_{-\infty}^{\infty} \mathrm{d}k \ \sqrt{\hbar\omega_{\alpha k}}\, \hat{a}_{\alpha k} \bar{\mathbf{d}}_{\alpha k} \exp(\mathrm{i}kz) + \mathrm{h.c.},$$

$$\hat{S}^{ij} = \sum_{\beta} \frac{1}{2\sqrt{\pi}} \int_{-\infty}^{\infty} \mathrm{d}q \ \sqrt{\hbar\Omega_{\beta q}}\, \hat{b}_{\beta q} \bar{s}^{ij}_{\beta q} \exp(\mathrm{i}qz) + \mathrm{h.c.},$$

with 'h.c.' representing the Hermitian conjugate. Here, $\bar{\mathbf{d}}_{\alpha k}$ is the electric induction field of the αth classical optical eigenmode with wave number k and has been normalized according to

$$\bar{\mathbf{d}}_{\alpha k} = \left[\int \mathrm{d}^2 r \ \frac{\mathbf{d}^*_{\alpha k} \cdot \mathbf{d}_{\alpha k}}{\varepsilon_{\mathrm{r}}(x, y)\varepsilon_0} \right]^{-\frac{1}{2}} \mathbf{d}_{\alpha k} = \sqrt{\frac{2}{\mathcal{E}_{\alpha k}}}\, \mathbf{d}_{\alpha k}, \tag{2}$$

where $\mathbf{d}_{\alpha k}$ is an arbitrary solution to the classical optical wave equation and $\mathcal{E}_{\alpha k}$ its classical energy per unit length of the waveguide [24]. Analogously, the modal strain field $\bar{s}^{ij}_{\beta q}$ associated with wave number q and mode index β is normalized to its classical energy $\mathcal{E}_{\beta q}$ per unit length of waveguide [24]:

$$\bar{s}^{ij}_{\beta q} = \sqrt{\frac{2}{\mathcal{E}_{\beta q}}}\, s^{ij}_{\beta q}. \tag{3}$$

Note that in the original Hamiltonian formulation [29], the optical and acoustic modal fields were each normalized to carry a single quantum per unit waveguide length, as opposed to the arbitrary normalization we allow here. The two pictures can be connected by choosing $\mathcal{E}_{\alpha k} = \hbar\omega_{\alpha k}$ and $\mathcal{E}_{\beta q} = \hbar\Omega_{\beta k}$.

To obtain a representation suitable for describing pulse propagation, we transform to the spatial domain by introducing envelope operators $\hat{\psi}_{\alpha}(z, t)$, $\hat{\phi}_{\beta}(z, t)$

$$\hat{\psi}_{\alpha}(z, t) = \frac{1}{\sqrt{2\pi}} \int_{-\infty}^{\infty} \mathrm{d}k \ \hat{a}_{\alpha k}(t) \exp(\mathrm{i}kz), \tag{4}$$

$$\hat{\phi}_{\beta}(z, t) = \frac{1}{\sqrt{2\pi}} \int_{-\infty}^{\infty} \mathrm{d}q \ \hat{b}_{\beta q}(t) \exp(\mathrm{i}qz), \tag{5}$$

and propagation operators $\mathcal{L}_{\alpha}$ and $\mathcal{L}_{\beta}$:

$$\mathcal{L}_{\alpha} = \hbar\omega_0 + \hbar \sum_{n=1}^{\infty} \frac{(-\mathrm{i})^n}{n!} \nu_{\alpha}^{(n)} (\partial_z - \mathrm{i}k_{\alpha})^n, \tag{6}$$

$$\mathcal{L}_{\beta} = \hbar\Omega_{\beta q_0} + \hbar \sum_{n=1}^{\infty} \frac{(-\mathrm{i})^n}{n!} \nu_{\beta}^{(n)} (\partial_z - \mathrm{i}q_{\beta})^n, \tag{7}$$

where we explicitly assume that all optical carriers have the same frequency ω_0, because in basically every experiment the optical frequency is defined by the vacuum wave length of the used laser; the different optical wave numbers and the wave numbers and frequencies of the excited acoustic modes follow from this frequency via the optical and acoustic dispersion relations. The first ($n = 1$) elements in each set of coefficients

$$\nu_{\alpha}^{(n)} = \left. \frac{\partial^n \omega_{\alpha k_{\alpha}}}{\partial k^n} \right|_{k_{\alpha}}, \qquad \nu_{\beta}^{(n)} = \left. \frac{\partial^n \Omega_{\beta q_{\beta}}}{\partial q^n} \right|_{q_{\beta}} \tag{8}$$

are the optical and acoustic acoustic group velocities, respectively. Their products with the modal energies $\mathcal{E}$ per unit length of waveguide are the modal powers through the transversal waveguide plane:

$$\mathcal{P}_{\alpha} = \nu_{\alpha}^{(1)} \mathcal{E}_{\alpha}, \qquad \mathcal{P}_{\beta} = \nu_{\beta}^{(1)} \mathcal{E}_{\beta}.$$

The operator $\mathcal{L}_{\alpha}$ emerges from equation (1) by expressing the optical dispersion relation $\omega_{\alpha k}$ as a Taylor series in k and by substituting

$$k \to -\mathrm{i}\partial_z,$$

in the course of the Fourier transformation to the real-space representation. The operator $\mathcal{L}_{\beta}$ is defined likewise for the acoustic dispersion relation. This description is based on the convergence of the k-space Taylor series and is therefore valid inside a disk in complex k-space where the radius is determined by the nearest complex point of degeneracy (found at band crossings and near anti-crossing). The operators $\hat{\phi}_{\alpha}$ and $\hat{\psi}_{\beta}$ are fast operators in the sense that they oscillate according to $\exp(\mathrm{i}k_{\alpha}z)$ and $\exp(\mathrm{i}q_{\beta}z)$, respectively. They have dimensions of $1/\sqrt{\text{length}}$ and fulfill the commutation relations

$$[\hat{\psi}_{\alpha}(z), \hat{\psi}^{\dagger}_{\alpha'}(z')] = \delta_{\alpha\alpha'}\delta(z - z'), \tag{9}$$

$$[\hat{\phi}_{\beta}(z), \hat{\phi}^{\dagger}_{\beta'}(z')] = \delta_{\beta\beta'}\delta(z - z'). \tag{10}$$

This differs from the formally very similar operators introduced for each individual Stokes order by Sipe and Steel [29]. The difference is that the integrals in equations (4) and (5) formally cover the complete k-range instead of small k-space intervals of width $\Delta k \approx \Omega/v_\alpha$ as in [29].

Our first approximation is an SVEA: the field distributions are approximated as modulations of the carrier eigenmodes

$$\hat{\mathbf{D}} \approx \sum_\alpha \sqrt{\frac{\hbar\omega_0}{2}}\,\bar{\mathbf{d}}_{\alpha k_\alpha}\hat{\psi}_\alpha + \text{h.c.}, \tag{11}$$

$$\hat{S}^{ij} \approx \sum_\beta \sqrt{\frac{\hbar\,\Omega_{\beta q_\beta}}{2}}\,\bar{s}^{ij}_{\beta q_\beta}\,\hat{\phi}_\beta + \text{h.c.}, \tag{12}$$

where we explicitly allow for envelopes that vary on a time scale shorter than the acoustic period (what we call a 'relaxed' SVEA). Equations (11) and (12) are justified if neither the optical dispersion relation nor the optical mode patterns vary appreciably over the wave number range of multiple Stokes shifts. This is usually the case away from special points in the dispersion relation such as band edges.

3.1. Hamiltonian

We now derive the interaction term that is appropriate for our choice of envelopes. Here, we focus on the electrostrictive interaction term in order to keep our equations short. Discussions of how to derive radiation pressure within a coupled-mode picture of SBS can be found in the literature [23, 24, 29]. The electrostrictive interaction term is [29]:

$$\mathcal{V} = \frac{1}{2\varepsilon_0}\int \mathrm{d}^3 r \sum_{ijkl} \hat{D}_i \hat{D}_j p_{ijkl} \hat{S}^{kl} \tag{13}$$

$$= \sum_{\beta,\alpha,\alpha'} \frac{\hbar\omega_0\sqrt{\hbar\,\Omega_{\beta q_\beta}}}{2\varepsilon_0\sqrt{8}} \int \mathrm{d}^3 r \sum_{ijkl} \{[\bar{d}^{\,i}_{\alpha k_\alpha}\hat{\psi}_\alpha + (\bar{d}^{\,i}_{\alpha k_\alpha})^*\hat{\psi}^\dagger_\alpha][\bar{d}^{\,j}_{\alpha' k_{\alpha'}}\hat{\psi}_{\alpha'} + (\bar{d}^{\,j}_{\alpha' k_{\alpha'}})^*\hat{\psi}^\dagger_{\alpha'}]$$
$$\times\, p_{ijkl}[\bar{s}^{kl}_{\beta q_\beta}\hat{\phi}_\beta + (\bar{s}^{kl}_{\beta q_\beta})^*\hat{\phi}^\dagger_\beta]\}, \tag{14}$$

where $p_{ijkl}(\mathbf{r})$ is the photoelastic tensor distribution. We now employ an optical RWA, i.e. we neglect the terms proportional to $\hat{\psi}_\alpha^2$ and $(\hat{\psi}^\dagger_\alpha)^2$, because these terms oscillate at twice the optical frequency and cannot excite the acoustic system. We do, however, retain terms describing off-resonant excitation at harmonics of the acoustic frequency. Within this approximation, we find:

$$\mathcal{V} = \frac{1}{2}\sum_{\beta,\alpha,\alpha'}\int_{-\infty}^{\infty} \mathrm{d}z\ (\bar{\Gamma}_{\alpha\alpha'\beta}\hat{\psi}_\alpha\hat{\psi}^\dagger_{\alpha'}\hat{\phi}_\beta + \bar{\Gamma}_{\alpha'\alpha\beta}\hat{\psi}^\dagger_\alpha\hat{\psi}_{\alpha'}\hat{\phi}_\beta + \text{h.c.}), \tag{15}$$

with the coupling coefficient

$$\bar{\Gamma}_{\alpha\alpha'\beta} = \sqrt{\frac{\hbar^3\omega_0^2\Omega_{\beta q_\beta}}{\mathcal{E}_\alpha\mathcal{E}_{\alpha'}\mathcal{E}_\beta}}\,Q^{\mathrm{pe}}_{\alpha\alpha'\beta}, \tag{16}$$

where $Q^{\mathrm{pe}}_{\alpha\alpha'\beta}$ is the transverse electrostrictive overlap integral involving conventional eigenmodes:

$$Q^{\mathrm{pe}}_{\alpha\alpha'\beta} = \frac{1}{\varepsilon_0}\int \mathrm{d}^2 r \sum_{ijkl} d^{\,i}_{\alpha k_\alpha}\,(d^{\,j}_{\alpha' k_{\alpha'}})^* p_{ijkl} s^{kl}_{\beta q_\beta}. \tag{17}$$

This integral is only defined up to a phase factor that is given by the arbitrary global phase of the acoustic eigenmode. $Q^{\mathrm{pe}}_{\alpha\alpha'\beta}$ and as a result $\bar{\Gamma}_{\alpha\alpha'\beta}$ can be chosen to be real-valued for one pair of optical modes α and α' (but not necessarily for all pairs of optical modes at once). The addition of radiation pressure leads to the same result except for the addition of a surface integral $Q^{\mathrm{mb}}_{\alpha\alpha'\beta}$ to the total opto-acoustic overlap term $Q_{\alpha\alpha'\beta}$. This is well documented in the literature [23, 24, 29] and therefore need not be repeated here. The total Hamiltonian for the FBS problem is thus

$$\mathcal{H} = \sum_\alpha \int_{-\infty}^{\infty} \mathrm{d}z\ \hat{\psi}^\dagger_\alpha \mathcal{L}_\alpha \hat{\psi}_\alpha + \sum_\beta \int_{-\infty}^{\infty} \mathrm{d}z\ \hat{\phi}^\dagger_\beta \mathcal{L}_\beta \hat{\phi}_\beta$$
$$+ \frac{1}{2}\sum_{\beta,\alpha,\alpha'}\int_{-\infty}^{\infty} \mathrm{d}z\ (\bar{\Gamma}_{\alpha\alpha'\beta}\hat{\psi}_\alpha\hat{\psi}^\dagger_{\alpha'}\hat{\phi}_\beta + \bar{\Gamma}_{\alpha'\alpha\beta}\hat{\psi}^\dagger_\alpha\hat{\psi}_{\alpha'}\hat{\phi}_\beta + \text{h.c.}). \tag{18}$$

If desired, the optical operators in the interaction term can be normal-ordered:

$$\hat{\psi}_\alpha\hat{\psi}^\dagger_{\alpha'} = \hat{\psi}^\dagger_{\alpha'}\hat{\psi}_\alpha + [\hat{\psi}_\alpha, \hat{\psi}^\dagger_{\alpha'}], \tag{19}$$

where the commutator diverges according to equation (9), because it involves operators $\hat{\psi}_\alpha(z,\,t)$ and $\hat{\psi}^\dagger_{\alpha'}(z,\,t)$ evaluated at the same coordinate z. This only leads to a static deformation of the waveguide and is irrelevant for the dynamics of FBS. It can be interpreted as the contribution of the guided optical modes to the total Casimir force on the waveguide. We note that this force is not only restricted to boundary forces, but also has an electrostrictive contribution.

3.2. Equations of motion

The Heisenberg equations for the envelope operators are:

$$\begin{aligned}\partial_t\hat{\psi}_\alpha &= \frac{1}{\mathrm{i}\hbar}[\hat{\psi}_\alpha,\,\mathcal{H}]\\ &= \frac{1}{\mathrm{i}\hbar}\mathcal{L}_\alpha\hat{\psi}_\alpha + \frac{1}{2\mathrm{i}\hbar}\sum_{\alpha'\beta}[(\bar{\Gamma}_{\alpha\alpha'\beta}+\bar{\Gamma}_{\alpha'\alpha\beta})\hat{\phi}_\beta + (\bar{\Gamma}^*_{\alpha'\alpha\beta}+\bar{\Gamma}^*_{\alpha\alpha'\beta})\hat{\phi}^\dagger_\beta]\hat{\psi}_{\alpha'},\end{aligned} \tag{20}$$

$$\begin{aligned}\partial_t\hat{\phi}_\beta &= \frac{1}{\mathrm{i}\hbar}[\hat{\phi}_\beta,\,\mathcal{H}]\\ &= \frac{1}{\mathrm{i}\hbar}\mathcal{L}_\beta\hat{\phi}_\beta + \frac{1}{2\mathrm{i}\hbar}\sum_{\alpha\alpha'}(\bar{\Gamma}^*_{\alpha'\alpha\beta}\hat{\psi}_\alpha\hat{\psi}^\dagger_{\alpha'} + \bar{\Gamma}^*_{\alpha\alpha'\beta}\hat{\psi}^\dagger_\alpha\hat{\psi}_{\alpha'}).\end{aligned} \tag{21}$$

As we have already discussed, the commutator $[\hat{\psi}_{\alpha'},\,\hat{\psi}^\dagger_\alpha]$ is irrelevant for the dynamics of FBS and therefore it can be safely ignored:

$$\partial_t\hat{\phi}_\beta = \frac{1}{\mathrm{i}\hbar}\mathcal{L}_\beta\hat{\phi}_\beta + \frac{1}{2\mathrm{i}\hbar}\sum_{\alpha\alpha'}(\bar{\Gamma}^*_{\alpha'\alpha\beta}\hat{\psi}^\dagger_{\alpha'}\hat{\psi}_\alpha + \bar{\Gamma}^*_{\alpha\alpha'\beta}\hat{\psi}^\dagger_\alpha\hat{\psi}_{\alpha'}). \tag{22}$$

It is convenient to transform the optical operators to a rotating frame that eliminates both the temporal and the spatial carrier. It should be stressed that we do not apply such a transformation to the acoustic envelopes as this would lead to an explicitly time-dependent interaction term. Furthermore, the (nearly) vanishing acoustic group velocity suggests a rescaling to normalize with respect to energies rather than powers:

$$\hat{\Psi}_\alpha(z,\,t) = \hat{\psi}_\alpha(z,\,t)\sqrt{\hbar\omega_0}\,\exp(\mathrm{i}\omega_0 t - \mathrm{i}k_\alpha z), \tag{23}$$

$$\hat{\Phi}_\beta(z,\,t) = \hat{\phi}_\beta(z,\,t)\sqrt{\hbar\,\Omega_{\beta q_\beta}}, \tag{24}$$

$$\Gamma_{\alpha\alpha'\beta} = \frac{1}{\hbar\omega_0\sqrt{\hbar\,\Omega_{\beta q_\beta}}}\bar{\Gamma}_{\alpha\alpha'\beta} = \frac{1}{\sqrt{\mathcal{E}_\alpha\mathcal{E}_{\alpha'}\mathcal{E}_\beta}}Q_{\alpha\alpha'\beta}. \tag{25}$$

The product operators $\hat{\Psi}^\dagger\hat{\Psi}$ and $\hat{\Phi}^\dagger\hat{\Phi}$ thus express the local optical and acoustic energies rather than the local number of photons and phonons, respectively.

Using equations (6) and (7), the resulting quantum equations of motion are:

$$\begin{aligned}\left[\partial_t + v^{(1)}_\alpha\partial_z - \mathrm{i}\frac{v^{(2)}_\alpha}{2}\partial_z^2 + \cdots\right]\hat{\Psi}_\alpha = &-\frac{\mathrm{i}\omega_0}{2}\sum_{\alpha'\beta}\mathrm{e}^{\mathrm{i}(k_{\alpha'}-k_\alpha)z}[(\Gamma_{\alpha\alpha'\beta}+\Gamma_{\alpha'\alpha\beta})\hat{\Phi}_\beta\\ &+ (\Gamma^*_{\alpha\alpha'\beta}+\Gamma^*_{\alpha'\alpha\beta})\hat{\Phi}^\dagger_\beta]\hat{\Psi}_{\alpha'},\end{aligned} \tag{26}$$

$$\begin{aligned}\left[(\partial_t + \mathrm{i}\Omega_{\beta q_\beta}) + v^{(1)}_\beta(\partial_z - \mathrm{i}q_\beta) - \mathrm{i}\frac{v^{(2)}_\beta}{2}(\partial_z - \mathrm{i}q_\beta)^2 + \cdots\right]\hat{\Phi}_\beta = &-\frac{\mathrm{i}\Omega_{\beta q_\beta}}{2}\sum_{\alpha\alpha'}[\mathrm{e}^{\mathrm{i}(k_{\alpha'}-k_\alpha)z}\Gamma^*_{\alpha'\alpha\beta}\hat{\Psi}^\dagger_\alpha\hat{\Psi}_{\alpha'}\\ &+ \mathrm{e}^{\mathrm{i}(k_\alpha-k_{\alpha'})z}\Gamma^*_{\alpha\alpha'\beta}\hat{\Psi}^\dagger_{\alpha'}\hat{\Psi}_\alpha)].\end{aligned} \tag{27}$$

In most situations a classical description is sufficient and allows for the simple inclusion of loss via damping coefficients γ_α and γ_β. To this end, we identify the expectation value of the QM energy density operator with the classical energy density of modulated modes:

$$\langle\hat{\Psi}^\dagger_\alpha\hat{\Psi}_\alpha\rangle = \mathcal{E}_\alpha|a_\alpha|^2, \qquad \langle\hat{\Phi}^\dagger_\beta\hat{\Phi}_\beta\rangle = \mathcal{E}_\beta|\tilde{b}_\beta|^2, \tag{28}$$

where $a_\alpha(z,\,t)$ and $\tilde{b}_\beta(z,\,t)$ are classical dimensionless envelope functions. The tilde indicates that the acoustic envelopes are subject to a different phase convention than the optical envelopes. The classical equations of motion are therefore obtained from equations (26) and (27) by identifying:

$$\hat{\Psi}_\alpha \to \sqrt{\mathcal{E}_\alpha}\,a_\alpha, \qquad \hat{\Phi}_\beta \to \sqrt{\mathcal{E}_\beta}\,\tilde{b}_\beta; \tag{29}$$

$$\left[\gamma_\alpha + \partial_t + v_\alpha^{(1)}\partial_z - \mathrm{i}\frac{v_\alpha^{(2)}}{2}\partial_z^2 + \cdots\right]a_\alpha = -\frac{\mathrm{i}\omega_\alpha k_\alpha}{\mathcal{E}_\alpha}\sum_{\alpha'\beta}\mathrm{e}^{\mathrm{i}(k_{\alpha'}-k_\alpha)z} \times \Re\{(Q_{\alpha\alpha'\beta} + Q_{\alpha'\alpha\beta})\tilde{b}_\beta\}a_{\alpha'}, \tag{30}$$

$$\left[\gamma_\beta + (\partial_t + \mathrm{i}\Omega_{\beta q_\beta}) + v_\beta^{(1)}(\partial_z - \mathrm{i}q_\beta) - \mathrm{i}\frac{v_\beta^{(2)}}{2}(\partial_z - \mathrm{i}q_\beta)^2 + \cdots\right]\tilde{b}_\beta = -\frac{\mathrm{i}\Omega_{\beta q_\beta}}{2\mathcal{E}_\beta}\sum_{\alpha\alpha'}(\mathrm{e}^{\mathrm{i}(k_{\alpha'}-k_\alpha)z}Q^*_{\alpha'\alpha\beta}a^*_\alpha a_{\alpha'} + \mathrm{e}^{\mathrm{i}(k_\alpha-k_{\alpha'})z}Q^*_{\alpha\alpha'\beta}a^*_{\alpha'}a_\alpha). \tag{31}$$

Note that the optical damping coefficient is defined with respect to amplitudes and not powers. Thus, it satisfies $\gamma_\alpha = v_\alpha\alpha_{\mathrm{loss}}/2$, where α_{loss} is the conventional power attenuation coefficient.

The framework presented thus far is directly applicable intra-mode FBS—which is the main focus of this paper—and for non-cascaded inter-mode backward SBS. The treatment of cascaded inter-mode FBS and intra-mode backward SBS requires *two* carriers either in an acoustic or in an optical mode in order to describe forward and backward propagating acoustic waves (in the case of inter-mode FBS) or forward and backward propagating optical waves (in the case of intra-mode backward SBS).

3.3. Intra-mode FBS

Often, only one optical mode $\alpha = \alpha'$ and one acoustic mode β are relevant. In this case, the coefficients simplify and phase factors disappear:

$$Q_{\alpha\alpha'\beta} = Q_{\alpha'\alpha\beta} = Q, \tag{32}$$

$$\mathrm{e}^{\mathrm{i}(k_{\alpha'}-k_\alpha)z} = \mathrm{e}^{\mathrm{i}(k_\alpha-k_{\alpha'})z} = 1, \tag{33}$$

the mode-index summations in the interaction terms disappear and we drop the subscripts α, β, k_α and q_β where appropriate and use k_0, Ω_0, and q_0 to denote the optical and acoustic carrier wave parameters. This leads to simplified quantum equations of motion

$$[\partial_t + v_\alpha^{(1)}\partial_z + \cdots]\hat{\Psi} = -\mathrm{i}\omega_0(\Gamma\hat{\Phi} + \Gamma^*\hat{\Phi}^\dagger)\hat{\Psi}, \tag{34}$$

$$[(\partial_t + \mathrm{i}\Omega_0) + v_\beta^{(1)}(\partial_z - \mathrm{i}q_0) + \cdots]\hat{\Phi} = -\mathrm{i}\Omega_0\Gamma^*\hat{\Psi}^\dagger\hat{\Psi}, \tag{35}$$

and their classical counterparts:

$$[\gamma_\alpha + \partial_t + v_\alpha^{(1)}\partial_z + \cdots]a = -\frac{2\mathrm{i}\omega_0}{\mathcal{E}_\alpha}\Re\{Q\tilde{b}\}a, \tag{36}$$

$$[\gamma_\beta + (\partial_t + \mathrm{i}\Omega_0) + v_\beta^{(1)}(\partial_z - \mathrm{i}q_0) + \cdots]\tilde{b} = -\frac{\mathrm{i}\Omega_0}{\mathcal{E}_\beta}Q^*|a|^2. \tag{37}$$

The remainder of this paper is entirely based on the classical equations of motion with only one relevant optical and one relevant acoustic mode.

We now demonstrate how the equations (30) and (31) can be reduced to the standard treatment with individual optical amplitudes for each Stokes order. First, we assume that the optical amplitude can be represented as a superposition of a pump and N Stokes and M anti-Stokes orders:

$$a(z,t) = \sum_{n=-M}^{N} a_n(z,t)\exp[-\mathrm{i}n(\Omega_0 - q_0 z t)], \tag{38}$$

where each individual amplitude a_n is assumed to vary slowly on the time and length scales of the *acoustic* problem. Furthermore, it is now convenient to transform the acoustic envelope to a rotating frame:

$$b(z,t) = \tilde{b}(z,t)\exp(\mathrm{i}\Omega_0 t - \mathrm{i}q_0 z). \tag{39}$$

We insert this into equation (30) to obtain:

$$0 = \sum_{n=-M}^{N}\left\{\mathrm{e}^{\mathrm{i}n(\mathrm{i}\Omega_0 t - q_0 z)}\left[\gamma_\alpha + (\partial_t - \mathrm{i}n\Omega_0) + v_\alpha^{(1)}(\partial_z + \mathrm{i}nq_0) - \mathrm{i}\frac{v_\alpha^{(2)}}{2}(\partial_z^2 + 2n\mathrm{i}q_0\partial_z - n^2q_0^2) + \cdots\right]a_n + \frac{\mathrm{i}\omega_0}{\mathcal{E}_\alpha}[\mathrm{e}^{\mathrm{i}(n+1)(\mathrm{i}\Omega_0 t - q_0 z)}Qb + \mathrm{e}^{\mathrm{i}(n-1)(\mathrm{i}\Omega_0 t - q_0 z)}Q^*b^*]a_n\right\}. \tag{40}$$

Given the slowly varying constraint, this equation is equivalent to a family of equations for the individual Stokes orders:

$$[\gamma_\alpha + (\partial_t - \mathrm{i}n\Omega_0) + \nu_\alpha^{(1)}(\partial_z + \mathrm{i}nq_0) + \cdots]a_n = -\frac{\mathrm{i}\omega_0}{\mathcal{E}_\alpha}(Qba_{n-1} + Q^*b^*a_{n+1}), \tag{41}$$

with the truncation condition

$$a_{-M-1} = a_{N+1} = 0. \tag{42}$$

Analogously, we now insert the optical decomposition into the acoustic equation of motion (30):

$$\left[\gamma_\beta + \partial_t + \nu_\beta^{(1)}\partial_z - \mathrm{i}\frac{\nu_\beta^{(2)}}{2}\partial_z^2 + \cdots\right]b = -\frac{\mathrm{i}\Omega_0 Q^*}{\mathcal{E}_\beta}\sum_{n=-M}^{N-1} a_n^* a_{n+1} + \text{non-resonant terms}, \tag{43}$$

where 'non-resonant terms' contains all products of optical envelopes where the beating is not proportional to $\exp(\mathrm{i}q_0 z - \mathrm{i}\Omega_0 t)$. Neglecting these terms is equivalent to tightening the optical RWA to an acousto-optical RWA that ignores all contributions that disappear when averaged over a time scale much longer than the *acoustic* period. Equations (41)–(43) are the conventional coupled-mode equations for a large number of (anti-)Stokes orders.

The common case of a pump and a single Stokes side-band are obtained for $M = 0, N = 1$:

$$(\gamma_\alpha + \partial_t + \nu_\alpha^{(1)}\partial_z + \cdots)a_0 = -\frac{\mathrm{i}\omega_0 Q}{\mathcal{E}_\alpha}ba_1, \tag{44}$$

$$(\gamma_\alpha + \partial_t + \nu_\alpha^{(1)}\partial_z + \cdots)a_1 = -\frac{\mathrm{i}\omega_0 Q^*}{\mathcal{E}_\alpha}b^*a_0, \tag{45}$$

$$(\gamma_\beta + \partial_t + \nu_\beta^{(1)}\partial_z + \cdots)b = -\frac{\mathrm{i}\Omega_0 Q^*}{\mathcal{E}_\beta}a_1^*a_0, \tag{46}$$

where we have used the fact that the terms containing Ω_0 and q_0 cancel each other in equation (45) if the acoustic wave satisfies the phase-matching condition. The terms with Ω_0 and q_0 never appear in equation (44), because $n = 0$.

Equations (44)–(46) are in agreement with the literature on conventional classical coupled mode theory for SBS [23, 24]. With this, we have demonstrated that the commonly employed multi-envelope theory to FBS emerges from our treatment by restricting the assumptions about the optical spectrum and neglecting terms oscillating at multiples of the acoustic frequency in the interaction.

It should be remarked that higher-order dispersion terms (indicated by ellipses in equations (35)–(44)) are implicitly included and can lead to slight variations in the spacing between subsequent Stokes orders. In the case of a locally linear optical dispersion relation, the acoustic dispersion relation is irrelevant and the Stokes orders are uniformly spaced. For a locally curved optical band, any acoustic dispersion (including $\nu_\beta^{(1)}$) leads to the aforementioned varying spacing and non-local effects. A further discussion of this can be found see in section 6.3.

4. Complete analytical solution in dispersionless intra-mode FBS

Optical and acoustic dispersion are typically very small over the narrow frequency ranges (usually MHz to GHz) of Brillouin phenomena. Furthermore the propagation length of sound in a waveguide can be far smaller than the variation of the acoustic and optical envelopes, and so the propagation of acoustic waves is often neglected in Brillouin calculations. Having established the governing equations (30) and (31) we now examine the important limit where both optical and acoustic dispersion can be entirely neglected, and where the propagation length of acoustic waves is assumed to be equal to zero. We will see that this canonical situation provides insight, in the form of analytic solutions to the governing equations, into the overall behavior of FBS processes. In this section, we will solve the dispersionless initial value problem corresponding to equations (30) and (31) in this no-dispersion, no-acoustic-propagation limit:

$$(\partial_t + v\partial_z)a = -\left(\frac{2\mathrm{i}\omega_0}{\mathcal{E}_\alpha}\Re\{Q\tilde{b}\} + \gamma_\alpha\right)a, \tag{47}$$

$$(\partial_t + \gamma_\beta + \mathrm{i}\Omega_0)\tilde{b} = -\frac{\mathrm{i}\Omega_0 Q^*}{\mathcal{E}_\beta}|a|^2, \tag{48}$$

$$a(z = 0,\, t) = A(t), \tag{49}$$

$$a(z,\,t) = \tilde{b}(z,\,t) = A(t) = 0 \quad \text{for} \quad t < 0, \tag{50}$$

where $A(t)$ is the incident optical envelope at the start of the waveguide.

The general approach in solving this system is to first integrate the optical equation (47) to find the optical amplitude as a function of z and t. This solution will depend on the incident optical field $A(t)$ and the yet unknown acoustic envelope $\tilde{b}(z,\,t)$. We then insert it into equation (48) and find that the resulting equation happens to be solvable. By back-substitution into the solution to equation (47) we find the analytical solution to cascaded FBS as an explicit integral and evaluate it for a typical experimental setup.

4.1. General solution

Equation (47) is separable when integrating along the characteristic of the one-way wave equation. In other words, we obtain the phase of the optical amplitude at the point $(z,\,t)$ by integrating along a line $(z',\,t')$ in space time defined by

$$z' = z - vs, \qquad t' = t - s, \tag{51}$$

where s is the running parameter. This leads to the solution (expressed in the original coordinates):

$$a(z,\,t) = A\left(t - \frac{z}{v}\right)\exp\left(-\frac{\gamma_\alpha z}{v}\right) \times \exp\left[\frac{2\omega_0}{\mathrm{i}\mathcal{P}_\alpha}\int_0^z \mathrm{d}z'\,\Re\left\{Q\tilde{b}\left(z',\,t - \frac{z - z'}{v}\right)\right\}\right]. \tag{52}$$

It should be pointed out that the integrand is purely real-valued and thus the acoustic envelope only introduces a phase. In the absence of optical dispersion, the effect of the acoustic deformation on the optical wave is a pure phase modulation and the optical intensity does not depend on $\tilde{b}$. However, the only thing relevant for equation (48) is the optical intensity distribution:

$$|a(z,\,t)|^2 = \left|\,E\left(t - \frac{z}{v}\right)\right|^2 \exp\left(-\frac{2\gamma_\alpha z}{v}\right). \tag{53}$$

With this, equation (48) becomes an ordinary differential equation that can be explicitly solved via its Green function:

$$\tilde{b}(z,\,t) = \frac{\Omega_0 Q^*}{\mathrm{i}\mathcal{E}_\beta}\int_0^\infty \mathrm{d}t'\,\mathrm{e}^{-(\gamma_\beta + \mathrm{i}\Omega_0)t' - \frac{2\gamma_\alpha z}{v}}\left|\,A\left(t - t' - \frac{z}{v}\right)\right|^2, \tag{54}$$

This expression only depends on $A(t)$, but not on $a(z,\,t)$. Therefore, equation (52) is a simple integral rather than an integral equation. Furthermore, the z-integral in equation (52) is trivial. We find for the $\tilde{b}$-related term appearing under the z-integral:

$$-\Re\left\{Q\tilde{b}\left(z',\,t - \frac{z - z'}{v}\right)\right\} = \frac{\Omega_0|Q|^2}{\mathcal{E}_\beta}\int_0^\infty \mathrm{d}t'\,\mathrm{e}^{-\gamma_\beta t' - \frac{2\gamma_\alpha z'}{v}}\left|\,A\left(t - t' - \frac{z}{v}\right)\right|^2 \sin(\Omega_0 t'). \tag{55}$$

The stationary solution for the optical envelope of cascaded FBS in the dispersionless case and for any incident optical envelope $A(t)$ is therefore:

$$\begin{aligned} a(z,\,t) &= A\left(t - \frac{z}{v}\right)\exp\left\{-\frac{\gamma_\alpha z}{v} + \frac{\mathrm{i}\Omega_0\omega_0|Q|^2\left(1 - \mathrm{e}^{-\frac{2\gamma_\alpha z}{v}}\right)}{\gamma_\alpha\mathcal{E}_\alpha\mathcal{E}_\beta}\right. \\ &\quad \left.\times\int_0^\infty \mathrm{d}t'\,\mathrm{e}^{-\gamma_\beta t'}\left|\,A\left(t - t' - \frac{z}{v}\right)\right|^2 \sin(\Omega_0 t')\right\}, \\ &= A\left(t - \frac{z}{v}\right)\exp\left\{-\frac{\gamma_\alpha z}{v} + \frac{\mathrm{i}\Omega_0\omega_0|Q|^2}{\mathcal{E}_\alpha\mathcal{E}_\beta}\frac{2L_{\mathrm{eff}}}{v}\right. \\ &\quad \left.\times\int_0^\infty \mathrm{d}t'\,\mathrm{e}^{-\gamma_\beta t'}\left|\,A\left(t - t' - \frac{z}{v}\right)\right|^2 \sin(\Omega_0 t')\right\}, \end{aligned} \tag{56}$$

where the effective propagation length of the optical field at point z is

$$L_{\mathrm{eff}} = \frac{v\left(1 - \mathrm{e}^{-\frac{2\gamma_\alpha z}{v}}\right)}{2\gamma_\alpha}. \tag{57}$$

The resulting optical field can then be understood as the input field $A(t)$ attenuated according to the damping γ_a/v while being phase modulated by its own intensity over the effective length.

4.2. Example: two-tone excitation and zero optical loss

The explicit formula (56) is the complete solution to the problem of cascaded FBS in the absence of optical dispersion. To gain more insight into its nature, we next evaluate it for an example that is typical both for theoretical and experimental studies of SBS: the excitation with a strong optical pump and a weak Stokes side band:

$$A(t) = A_0[1 - \mathrm{i}M\exp(\mathrm{i}\Omega_0 t)], \tag{58}$$

where A_0 is the amplitude of the pump wave and MA_0 is that of the Stokes seed. The corresponding pump and Stokes seed powers are

$$P_\mathrm{P} = \mathcal{P}_\alpha|A_0|^2 \qquad P_\mathrm{S} = \mathcal{P}_\alpha|MA_0|^2 \tag{59}$$

We assume that M is real-valued, which is always possible by an appropriately chosen time origin. We furthermore neglect the optical loss γ_α in this specific example; the inclusion is straight-forward but tends to obscure the equations. On thus letting $L_\mathrm{eff} \to z$ and $\gamma_\alpha \to 0$, the solution becomes

$$a(z,t) = A\left(t - \frac{z}{v}\right)\exp\left\{\frac{2\mathrm{i}\Omega_0\omega_0|Q|^2 z}{\mathcal{P}_\alpha\mathcal{E}_\beta} \times \int_0^\infty \mathrm{d}t'\, \mathrm{e}^{-\gamma_\beta t'}\left|A\left(t - t' - \frac{z}{v}\right)\right|^2 \sin(\Omega_0 t')\right\} \tag{60}$$

$$= A\left(t - \frac{z}{v}\right)\exp\left\{\underbrace{\frac{2\mathrm{i}\Omega_0^2\omega_0|Q|^2(P_\mathrm{P}+P_\mathrm{S})z}{\mathcal{P}_\alpha^2\mathcal{E}_\beta(\gamma_\beta^2+\Omega_0^2)}}_{\text{static term}} + -\frac{2\mathrm{i}\Omega_0\omega_0|Q|^2\sqrt{P_\mathrm{P}P_\mathrm{S}}z}{\gamma_\beta\mathcal{P}_\alpha^2\mathcal{E}_\beta}\left[\underbrace{\cos\left(\Omega_0 t - \frac{\Omega_0 z}{v}\right)}_{\text{dominant term}}\right.\right.$$

$$\left.\left. + \underbrace{\frac{\gamma_\beta \mathrm{e}^{-\mathrm{i}\Omega_0(t-z/v)}}{2(\gamma_\beta - 2\mathrm{i}\Omega_0)} + \frac{\gamma_\beta \mathrm{e}^{\mathrm{i}\Omega_0(t-z/v)}}{2(\gamma_\beta + 2\mathrm{i}\Omega_0)}}_{\text{counter-rotating term}}\right]\right\}. \tag{61}$$

For high mechanical quality factors (i.e. $\Omega_0 \gg \gamma_\beta$), the additional phase factor due to static waveguide deformations and the out-of-phase contributions due to the counter-rotating term are negligible compared to the resonant effect. We introduce a natural unit of length that depends on the optical input powers and the intrinsic SBS parameters and we shift the origin of the time coordinate to a more convenient point:

$$\zeta = z/L_\mathrm{nat}, \tag{62}$$

$$\tau = t - \frac{z}{\Omega_0 v}, \tag{63}$$

$$\text{with} \quad L_\mathrm{nat} = \frac{\mathcal{P}_\alpha^2\mathcal{E}_\beta\gamma_\beta}{2\Omega_0\omega_0|Q|^2\sqrt{P_\mathrm{P}P_\mathrm{S}}} = \frac{1}{G_\mathrm{SBS}\sqrt{P_\mathrm{P}P_\mathrm{S}}}, \tag{64}$$

where G_SBS is the quantity that is often referred to as the 'SBS power gain' [24]. In these units, the cascaded FBS effect (excluding static deformations that only introduce a very slow phase factor $\exp(\mathrm{i}A\zeta)$ where A is approximately the inverse mechanical quality factor) takes a generic and simple form:

$$a(\zeta,\tau) = A(\tau)\exp[\mathrm{i}\zeta\cos(\Omega_0\tau)]. \tag{65}$$

We will now investigate three properties of this solution that are of particular interest for the characterization of SBS-based frequency combs: the frequency spectrum, the intensity evolution and the auto-correlation function.

The frequency spectrum of the total signal equation (65) is the convolution of the spectrum of the incident signal $A(\tau)$ and the SBS-modulation function

$$\mathcal{R}(\zeta,\tau) = \exp[\mathrm{i}\zeta\cos(\Omega_0\tau)], \tag{66}$$

which reflects the effect of cascaded FBS. Due to the periodicity of the problem, its spectrum only contains narrow lines at integer multiples of the Stokes shift Ω_0. Therefore, the spectral component of the nth (anti-) Stokes order is given by

$$\mathcal{R}_n(\zeta) = \frac{1}{2\pi}\int_0^{2\pi/\Omega_0} \mathrm{d}\tau\, \exp[\mathrm{i}n\Omega_0\tau + \mathrm{i}\zeta\cos(\Omega_0\tau)] \tag{67}$$

$$= \frac{1}{\Omega_0}J_n(\zeta), \tag{68}$$

where $J_n(\zeta)$ is the Bessel function of order n. We therefore can directly plot the generation of the individual Stokes orders along the waveguide (see figure 3). Cascaded FBS clearly generates a frequency comb in the sense

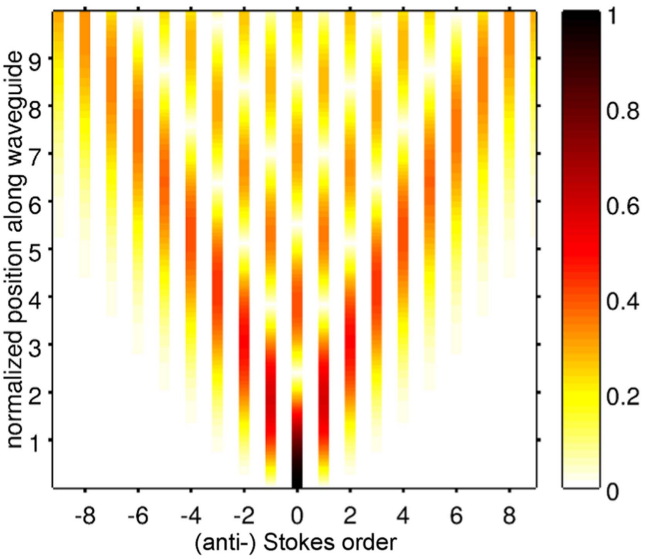

Figure 3. Evolution of the absolute amplitude (gray scale) of various (anti-)Stokes orders (frequency on the abscissa) as a function of position ζ along the wave guide (ordinate) assuming vanishing dispersion and an optical excitation with a strong pump and a weak Stokes side-band.

that it generates many equally spaced frequency lines. We note that this result is in agreement with theory presented in the supplementary material of [28].

However, very often frequency combs are associated with the generation of light pulses that are equally spaced in time domain. The solution of cascaded FBS in the absence of optical dispersion in a straight waveguide does not predict the formation of pulses. Even more, the SBS response function $\mathcal{R}(\zeta, \tau)$ is a pure phase factor, i.e. the FBS process does not affect the intensity distribution at all. A related feature of this is that (in the absence of optical loss and dispersion) the acoustic amplitude is constant along the waveguide: the sound wave is not amplified. This is in agreement with an earlier work on the optical single-pass gain of FBS structures [18]. As a result, the effect of cascaded FBS in the non-dispersive regime cannot be observed in the RF-domain by detecting the interference within the optical output with a photodetector.

Finally, auto-correlation measurements of optical combs are often used instead of measuring the time-dependence of the optical intensity in order to grade the quality of a frequency comb. It turns out that the cascaded FBS process in a dispersionless straight waveguide causes a pronounced auto-correlation peak despite the complete lack of intensity modulation. The amplitude auto-correlation for this problem with time period $T = 2\pi/\Omega_0$ can be defined as:

$$\mathcal{L}(\tau) = \frac{1}{T}\int_0^T \mathrm{d}\tau'\, \mathcal{R}^*(\zeta, \tau')\mathcal{R}(\zeta, \tau' + \tau) \tag{69}$$

$$= \frac{1}{T}\int_0^T \mathrm{d}\tau'\, \exp\{\mathrm{i}\zeta[\cos\Omega_0\tau' - \cos\Omega_0(\tau' + \tau)]\}$$

$$= J_0\left(2\zeta \sin\frac{\Omega_0\tau}{2}\right), \tag{70}$$

where $J_0(x)$ is the Bessel function of order zero. In figure 4 we show the absolute value squared of this result for a range of normalized waveguide lengths ζ.

4.3. Typical parameter ranges in experiments

The question that arises naturally at this point is which values of ζ are typical for various types of experiments, i.e. which ranges of the figures 3 and 4 can be observed in the laboratory. To this end, we consider the cases of a suspended silicon nanobeam and a microstructured silica fiber. According to equation (64), the range of observable ζ is given by the 'SBS power gain' and the product of input Stokes and pump power. Since power handling of a waveguide is usually limited by the total optical power (i.e. by the sum $P_\mathrm{P} + P_\mathrm{S}$), the maximal value for ζ can be found for the case $P_\mathrm{P} = P_\mathrm{S}$, although this does not imply a weak Stokes as assumed in figures 3 and 4.

First, we consider a suspended silicon nanobeam as presented in [27] with a nominal 'SBS power gain' of $G_\mathrm{SBS} \approx 6500\ \mathrm{W^{-1}\,m^{-1}}$, a maximal traveling optical power of $P_\mathrm{P} + P_\mathrm{S} \approx 30$ mW (i.e. $\sqrt{P_\mathrm{P}P_\mathrm{S}} \leqslant 15$ mW) and a waveguide length up to $L = 2.5$ mm. This results in a length unit of up to $L_\mathrm{nat} \approx 10$ mm and hence $\zeta \leqslant 0.25$, which is somewhat below the appearance of the additional sidebands in figure 3. A more recent experiment [33]

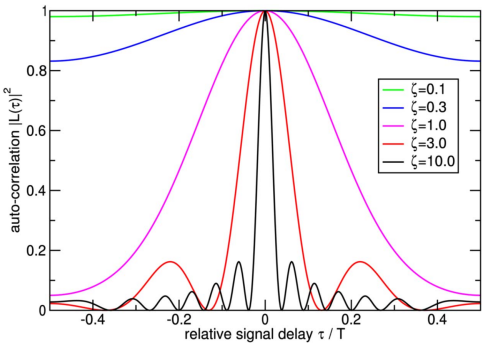

Figure 4. Absolute square $|\mathcal{L}(\tau)|^2$ of the auto-correlation function (see equation (69)) of the SBS-generated signal modulation $\mathcal{R}(\zeta, \tau)$ for a range of waveguide lengths ζ expressed in natural units of length L_{nat} (see equation (64)). The delay parameter τ is normalized to the acoustic period $T = 2\pi/\Omega_0$.

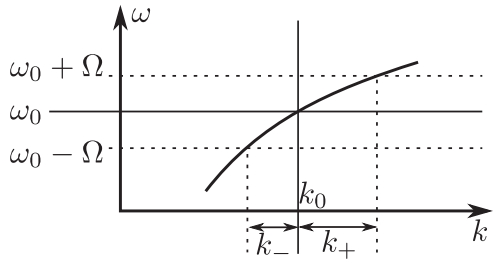

Figure 5. Sketch of a dispersive optical band. Three points are highlighted: a carrier wave at ω_0 and k_0, an anti-Stokes wave at $\omega_0 + \Omega_0$ and $k_0 + k_+$ and a Stokes wave at $\omega_0 - \Omega_0$ and $k_0 + k_-$ (note that k_- is chosen to be negative).

with $G_{\mathrm{SBS}} \approx 1000\ \mathrm{W}^{-1}\,\mathrm{m}^{-1}$ and $\sqrt{P_{\mathrm{P}} P_{\mathrm{S}}} \leqslant 30$ mW corresponds to a length unit of up to $L_{\mathrm{nat}} \approx 30$ mm. Given a total waveguide length of 80 mm, which is feasible because of the extremely low optical loss of the design, this device can operate at up to $\zeta \approx 2.5$ and therefore should exhibit signs of cascaded FBS given optimal levels of pump and input Stokes power. Finally, we consider a microstructured fiber as discussed in [28] with a nominal 'SBS power gain' of $G_{\mathrm{SBS}} \approx 1.5\mathrm{W}^{-1}\,\mathrm{m}^{-1}$ and pump powers around $P_{\mathrm{P}} \approx 500$ mW resulting in $L_{\mathrm{nat}} = 2.7$ m. Given that fibers can be fabricated with lengths of several 100 m and can have low optical loss, very large values of ζ can be realized in microstructured fibers.

5. Intra-mode FBS in dispersive waveguides

In the previous section, we have shown that in the absence of optical dispersion our cascaded model of FBS does not exhibit variations in the acoustic amplitude nor the intensity modulation along the waveguide. This is in fact not due to some hidden assumptions within our model but the result of the conservation of momentum and energy, i.e. phase matching. To illustrate this, we assume a waveguide that is acoustically modulated with the angular frequency Ω_0 and ask how the forward-scattering of light by this modulation modifies the acoustic intensity.

Figure 5 shows schematically a small section of an optical dispersion relation: a pump field at angular frequency ω_0 and wave number k_0 is scattered into the Stokes and anti-Stokes side bands at angular frequencies $\omega_0 \mp \Omega_0$ and wave numbers $k_0 + k_{\mp}$. The wave number differences can be expanded in terms of the frequency:

$$k_{\pm} = \pm s^{(1)}\Omega_0 + \frac{s^{(2)}}{2}\Omega_0^2 + \cdots, \tag{71}$$

where the group slowness and slowness dispersion parameters are connected to the more familiar group velocity and dispersion parameters (equation (8)) via:

$$s^{(1)} = [v^{(1)}]^{-1}, \qquad s^{(2)} = -v^{(2)}[v^{(1)}]^{-3}. \tag{72}$$

When part of the optical pump at ω_0 is scattered, its energy and momentum are distributed between the acoustic system and the two optical side bands expressed by amplitudes a_- and a_+ at the Stokes and anti-Stokes frequencies, respectively.

First, we will find a condition for the case that the acoustic amplitude is not modified, i.e. that the energy and momentum are distributed only among the optical side bands:

$$\hbar k_+|a_+|^2 + \hbar k_-|a_-|^2 = 0, \tag{73}$$

$$\hbar\Omega_0|a_+|^2 - \hbar\Omega_0|a_-|^2 = 0. \tag{74}$$

This is only possible if $k_+ = -k_-$, i.e. for vanishing optical dispersion (note that the acoustic wave number $q = k_+$ is not zero). In addition, we find that $|a_+|^2 = |a_-|^2$, i.e. that both side bands are equally excited in agreement with section 4. Finally, we may conclude that in the presence of optical dispersion, a two-wave process is not sufficient to simultaneously conserve energy and momentum, i.e. the acoustic system is required as a third participating wave.

Next, we we introduce B as the (positive or negative) change in the acoustic intensity $|b|^2$. The conservation of energy requires:

$$\hbar\Omega_0|a_+|^2 - \hbar\Omega_0|a_-|^2 + \hbar\Omega_0 B = 0, \tag{75}$$

$$\Rightarrow \quad B = |a_-|^2 - |a_+|^2. \tag{76}$$

Self-amplification occurs if energy is dumped into the acoustic field, i.e. for $B > 0$. For the conservation of momentum, we find:

$$\hbar k_+|a_+|^2 + \hbar k_-|a_-|^2 + \hbar q B = 0, \tag{77}$$

$$\Rightarrow \quad \frac{s^{(2)}\Omega_0^2}{2}(|a_-|^2 + |a_+|^2) + (q - s^{(1)}\Omega_0)B = 0. \tag{78}$$

From this we can see that a change in the acoustic intensity is necessary in the presence of optical dispersion. Furthermore, we can see that (unlike in the dispersionless case) the acoustic phase velocity must slightly differ form the optical group velocity.

This very simple argument based on the conservation of energy and momentum alone demonstrates that dispersion is necessarily required to modify the acoustic intensity via FBS. However, it cannot predict in which regime self-amplification occurs, because no assumptions are made about the opto-acoustic interaction. This requires a more detailed approach, as we will show in the following.

5.1. Amplification and suppression in the weak dispersion limit

We now study the full problems of FBS with optical dispersion, where we neglect optical loss for the sake of simplicity:

$$\left(\partial_t + v_\alpha^{(1)}\partial_z - \frac{\mathrm{i}v_\alpha^{(2)}}{2}\partial_z^2\right)a = \frac{2\mathrm{i}\omega_0}{\mathcal{E}_\alpha}\Re\{Q\tilde{b}\}a, \tag{79}$$

$$(\partial_t + \gamma_\beta + \mathrm{i}\Omega_0)\tilde{b} = -\frac{\mathrm{i}\Omega_0 Q^*}{\mathcal{E}_\beta}|a|^2, \tag{80}$$

$$a(z = 0,\, t) = A(t), \tag{81}$$

$$a(z,\, t) = b(z,\, t) = A(t) = 0 \quad \text{for} \quad t < 0. \tag{82}$$

In this problem, the optical dispersion gradually shifts the phase between adjacent Stokes lines with propagation along z and therefore slowly converts the pure phase-modulation of the opto-acoustic interaction into a partial amplitude-modulation. Depending on the sign of this process, the optical interference pattern is amplified or attenuated along the waveguide. Unfortunately, the parabolic nature of the optical equation precludes a closed form solution similar to equation (56). We therefore restrict ourselves to a few relevant aspects of the problem.

First, we eliminate constants that only clutter the notation by substituting

$$f(z,\, t) = \frac{|Q|}{\sqrt{\mathcal{E}_\alpha\mathcal{E}_\beta}}a(z,\, t), \tag{83}$$

$$g(z,\, t) = -\frac{Q}{\mathcal{E}_\alpha}\tilde{b}(z,\, t), \tag{84}$$

and by introducing the symbols $v = v_\alpha^{(1)}$ and $w = v_\alpha^{(2)}/2$. This leads to the equivalent equations:

$$[\mathrm{i}\partial_t + \mathrm{i}v\partial_z + w\partial_z^2 + \omega_0(g + g^*)]f = 0, \tag{85}$$

$$(\partial_t + \gamma_\beta + \mathrm{i}\Omega_0)g = \mathrm{i}\Omega_0|f|^2. \tag{86}$$

In the case of weak dispersion ($w \approx 0$), an approximate solution to equations (85) and (86) over a short length of waveguide ($z \approx 0$) can be found via first order perturbation theory. To this end, we first make the ansatz

$$f(z,\,t) = \exp[h(z,\,t) + \mathrm{i}j(z,\,t)], \tag{87}$$

with real-valued functions $h(z,\,t)$ and $j(z,\,t)$. Inserting this into equation (85) and separating real and imaginary parts of this equation, we reach the system

$$(\partial_t + \gamma_\beta + \mathrm{i}\Omega_0)g = \mathrm{i}\Omega_0 \mathrm{e}^{2h}, \tag{88}$$

$$\partial_t h + [v + 2w(\partial_z j)]\partial_z h = -w\partial_z^2 j, \tag{89}$$

$$(\partial_t + v\partial_z)j + w[(\partial_z j)^2 - (\partial_z h)^2 - \partial_z^2 h] = \omega_0(g + g^*). \tag{90}$$

We then write the exact function h (j and g likewise) as an expansion:

$$h(z,\,t) = h_0(z,\,t) + h_1(z,\,t) + h_2(z,\,t) + \cdots, \tag{91}$$

where h_0 is the solution to the dispersionless problem, h_n are the nth-order corrections corresponding to the powers w^n, and we will truncate after the first order term. As in the dispersionless solution, we take our previous result from section 4.2:

$$g_0(z,\,t) = \mathrm{i}G_0 \exp\left(-\mathrm{i}\Omega_0 \frac{vt - z}{v}\right), \tag{92}$$

$$h_0(z,\,t) = \log|F_0| + \log\left|1 - \mathrm{i}M\mathrm{e}^{\frac{\mathrm{i}\Omega_0(vt-z)}{v}}\right|, \tag{93}$$

$$j_0(z,\,t) = \frac{2G_0\omega_0 z}{v}\sin\left(\Omega_0 \frac{vt - z}{v}\right), \tag{94}$$

where

$$F_0 = \frac{|Q|A_0}{\sqrt{\mathcal{E}_\alpha \mathcal{E}_\beta}} \tag{95}$$

is the transformed optical mean amplitude and we have omitted overall meaningless phase factors due to static deformation in order to keep the equations concise. The intensity modulation depth M is assumed to be small and connected to the acoustic amplitude $G_0 = \mathrm{i}|F_0|^2 M\Omega_0/\gamma_\beta$.

Next, we calculate the first-order correction to h and its effect on g; the resulting correction to j is not relevant within this context and therefore not shown. The correction to h satisfies:

$$\partial_t h_1 + [v + 2w(\partial_z j_0)]\partial_z h_1 = -w\partial_z^2 j_0, \tag{96}$$

with the boundary condition at $z = 0$

$$h_1(0,\,t) = 0. \tag{97}$$

This leads to the first order correction expressions (the intermediate steps leading up to this result can be found in the appendix):

$$h_1(z,\,t) = \frac{w\omega_0\Omega_0 G_0}{v^4}\left[4vz\cos\left(\Omega_0 \frac{vt - z}{v}\right) + \Omega_0 z^2 \sin\left(\Omega_0 \frac{vt - z}{v}\right)\right], \tag{98}$$

$$g_1(z,\,t) \approx \frac{2\mathrm{i}w\omega_0\Omega_0^2 G_0|F_0|^2}{v^4\gamma_\beta}[4vz + \mathrm{i}\Omega_0 z^2]\mathrm{e}^{\mathrm{i}\Omega_0\frac{z-vt}{v}}, \tag{99}$$

where we have neglected any non-resonant excitation of the mechanical system. This is justified for high mechanical quality factors.

This means that to first approximation and over a small distance z the acoustic amplitude is modified by a relative factor of

$$\frac{g_1(z,\,t)}{g_0(z,\,t)} = \frac{2w\omega_0\Omega_0^2|F_0|^2(4vz + \mathrm{i}\Omega_0 z^2)}{v^4\gamma_\beta}. \tag{100}$$

This suggests to make the ansatz

$$g(z,\,t) = G(z)g_0(z,\,t), \tag{101}$$

$$\text{with} \quad G(\Delta z) \approx \frac{2w\omega_0\Omega_0^2|F_0|^2(4v\Delta z + \mathrm{i}\Omega_0\Delta z^2)}{v^4\gamma_\beta} \tag{102}$$

$$= (a\Delta z + b\Delta z^2). \tag{103}$$

For infinitesimally small Δz. We can then approximate a waveguide of finite length z as a concatenation of pieces of decreasing length Δz:

$$G(n\Delta z) \approx (1 + a\Delta z + b\Delta z^2)G[(n-1)\Delta z], \tag{104}$$

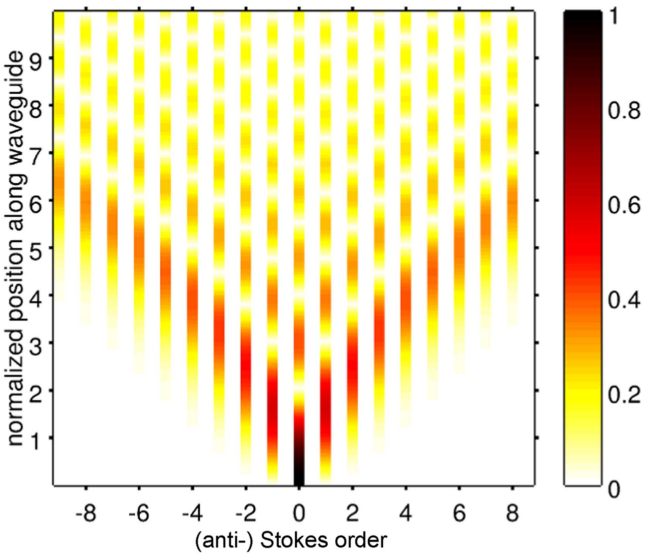

Figure 6. Evolution of the (anti-)Stokes orders for a normalized dispersion of $\bar{w} = -0.15$ assuming that the waveguide is long compared to the acoustic wave length and an optical excitation with a strong pump and a weak Stokes side-band (see also figure 3).

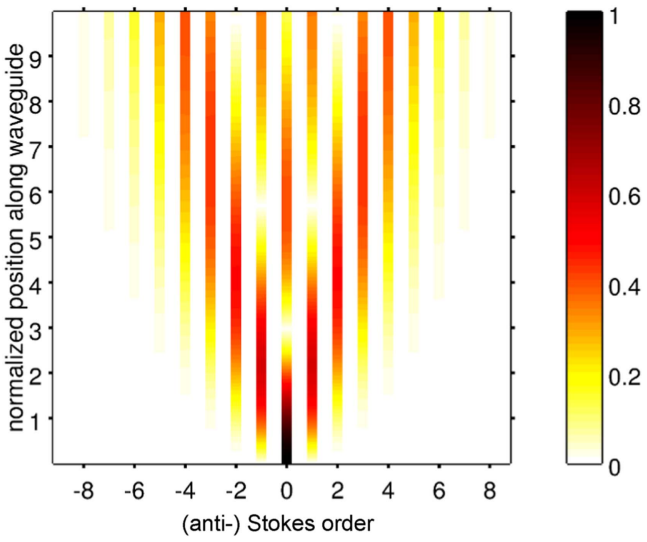

Figure 7. Evolution of the (anti-)Stokes orders for a normalized dispersion of $\bar{w} = 0.15$ assuming that the waveguide is long compared to the acoustic wave length and an optical excitation with a strong pump and a weak Stokes side-band (see also figure 3).

$$\Rightarrow G(z) = \lim_{z\to 0}[1 + a\Delta z + b\Delta z^2]^{z/\Delta z} \tag{105}$$

$$= \exp\left(\frac{8w\omega_0\Omega_0^2|F_0|^2}{\nu^3\gamma_\beta}z\right). \tag{106}$$

$$= \exp\left(\frac{8w\omega_0\Omega_0^2|Q|^2|A_0|^2}{\mathcal{P}_\alpha\mathcal{E}_\beta\nu^2\gamma_\beta}z\right). \tag{107}$$

This can be expressed in terms of the normalized length variable ζ by introducing a normalized dispersion parameter $\bar{w}$:

$$G(\zeta) = \exp(\bar{w}\zeta), \tag{108}$$

$$\text{with} \quad \bar{w} = \frac{4\Omega_0 w}{\nu^2}\sqrt{\frac{P_\mathrm{P}}{P_\mathrm{S}}}. \tag{109}$$

Figures 6 and 7, show the evolution of the optical spectrum along a waveguide for $\bar{w} = -0.15$ and $\bar{w} = +0.15$, respectively. This nicely illustrates that—within the bounds of this first-order perturbation theory, i.e. weak

dispersion, weak optical intensity contrast—the optical modulation pattern is compressed along z for $w > 0$ and stagnates for $w < 0$. The underlying reason for this is that anomalous dispersion translates the opto-acoustic phase modulation into an amplitude modulation with the same sign as the optical fluctuation that drives the acoustic oscillation. As a result, both the intensity modulation and the acoustic amplitude grow along the waveguide. In contrast, normal dispersion leads to an amplitude modulation that diminishes optical intensity fluctuations along the waveguide.

5.2. Connection of intra-mode FBS to Raman scattering and soliton dynamics

The formalism presented so far is particularly well suited for the combination of FBS with other optical nonlinearities, especially Raman-scattering and the Kerr effect. This is because the multi-Stokes optical envelope readily covers nonlinear interference terms between various Stokes orders, which have to be explicitly included in more conventional coupled mode theory [34] and would clutter the equations for cascaded Brillouin scattering [35]. The dynamics of solitons in optical fibers can be expressed by a retarded nonlinear Schroedinger equation, [30] where the instantaneous Kerr effect and Raman scattering enter through the convolution of the optical intensity with a (time-dependent) response function $r(t)$ as the convolution kernel. Our FBS equations of motion including this response function and for the complete set of mechanical modes read:

$$\left[\gamma_\alpha + \partial_t + \nu_\alpha^{(1)}\partial_z + \mathrm{i}\frac{\nu_\alpha^{(2)}}{2}\partial_z^2\right]a(z,\,t) = \left[\underbrace{\frac{2\omega_0}{\mathrm{i}\mathcal{E}_\alpha}\sum_\beta \Re\{Q_\beta \tilde{b}_\beta(z,\,t)\}}_{\text{FBS}} + \underbrace{\mathrm{i}\int_0^\infty \mathrm{d}t'\; r(t')|a(z,\,t-t')|^2}_{\text{Raman}}\right]a(z,\,t), \tag{110}$$

$$[\gamma_\beta + (\partial_t + \mathrm{i}\Omega_\beta) + \nu_\beta^{(1)}(\partial_z - \mathrm{i}q_0)]\tilde{b}_\beta(z,\,t) = -\frac{\mathrm{i}\Omega_\beta}{\mathcal{E}_\beta}Q_\beta^*|a(z,\,t)|^2. \tag{111}$$

The acoustic equations of motion can be formally solved using Green functions:

$$\tilde{b}_\beta(z,\,t) = -\frac{\mathrm{i}Q_\beta^*}{\mathcal{E}_\beta}\int_0^\infty \mathrm{d}t'\;|a(z-\nu_\beta t',\,t-t')|^2\mathrm{e}^{-(\gamma_\beta+\mathrm{i}\Omega_\beta-\mathrm{i}\nu_\beta^{(1)}q_0)t'}. \tag{112}$$

This allows us to combine the Raman kernel with the Brillouin response in a single function $r_{\mathrm{eff}}(z,\,t)$:

$$\left[\gamma_\alpha + \partial_t + \nu_\alpha^{(1)}\partial_z + \mathrm{i}\frac{\nu_\alpha^{(2)}}{2}\partial_z^2\right]a(z,\,t) = \mathrm{i}a(z,\,t)\int_0^\infty \mathrm{d}t'\;\int_0^\infty \mathrm{d}z'\; r_{\mathrm{eff}}(z',\,t')|a(z-z',\,t-t')|^2, \tag{113}$$

where the effective response function is spatially non-local due to the traveling nature of the sound waves in addition to the temporal non-locality that is known from Raman scattering:

$$r_{\mathrm{eff}}(z,\,t) = \delta(z)r(t) - \sum_\beta \frac{2\omega_0\Omega_\beta|Q_\beta|^2}{\mathcal{E}_\alpha\mathcal{E}_\beta}\mathrm{e}^{-\gamma_\beta t}\times\sin[(\Omega_\beta - \nu_\beta^{(1)}q_0)t]\;\delta(z-\nu_\beta^{(1)}t). \tag{114}$$

This spatial non-locality is the main difference between FBS and Raman scattering. This non-locality would be relevant for FBS involving a Dirac cone in the acoustic dispersion relation at $q = 0$. However, in practice FBS occurs at acoustic band edges, where the the acoustic group velocity $\nu_\beta^{(1)}$ so small that the phonon propagation length (i.e. the spatial non-locality) is but a few nanometers. In this case, spatial non-locality is negligible and intra-mode FBS can be regarded as a simple contribution to the low-frequency tail of the Raman spectrum:

$$r_{\mathrm{eff}}(t) = r(t) - \sum_\beta \frac{2\omega_0\Omega_\beta|Q_\beta|^2}{\mathcal{E}_\alpha\mathcal{E}_\beta}\mathrm{e}^{-\gamma_\beta t}\sin(\Omega_\beta t). \tag{115}$$

FBS can therefore be expected to contribute to the formation and the self-frequency shift of nanosecond-scale solitons in waveguides [30].

6. Discussion

After the analysis of the previous sections we now combine the results obtained in the different regimes and discuss their implications.

6.1. Phase modulation versus intensity modulation

We found in section 4, that intra-mode FBS without optical dispersion has a closed analytical solution in the form of a simple integral. One key observation within this result is that the acoustic field does not affect the optical intensity, i.e. neither the optical beat pattern nor the acoustic amplitude vary along the waveguide.

Consequently, dispersionless intra-mode FBS results only in a phase modulation of the optical signal. Thus, the acoustic amplitude is constant throughout the waveguide and the phase modulation grows linearly.

The situation changes fundamentally if the waveguide is dispersive. The optical dispersion slowly shifts the various (anti-)Stokes orders out of phase and thereby creates an FBS-related beating pattern, i.e. an optical intensity modulation. Depending on the sign of the dispersion constant, this new beating pattern can have the opposite or the same sign as the intensity fluctuation that drives the acoustic wave in the first place. In the former case, the total optical intensity variations (and thus the acoustic amplitude) diminish along the waveguide. However, the entropy of the fluctuating pump cannot disappear, so the reduction in the intensity modulation has to be countered by a phase modulation. In the other case (additive beat patterns), optical intensity fluctuations (as well as the acoustic amplitude) are amplified along the waveguide and both the intensity and the phase modulation grow exponentially along the waveguide. We note that, having used a perturbative approach to solve this problem, these results are strictly only valid for weak dispersion and weak intensity contrasts—this approximation will therefore break down as the Stokes grows to be comparable with the pump. Nevertheless these results can be expected to remain qualitatively valid even in the cases of strong dispersion and large intensity contrasts.

6.2. Measurement of FBS

FBS occurs in various fields such as PCFs or integrated silicon waveguides. These systems are typically studied with different experimental techniques because of the very dissimilar loss regimes, power handling and waveguide lengths. Most fiber experiments capture the modulation of the optical wave with high fidelity either by using an interferometric setup or by measuring in another polarization. They usually do not inject a dedicated Stokes seed and instead observe scattering from phonons that are either thermally excited or generated by the intensity noise of the pump laser. The long interaction lengths and power handling in fiber optics allows for complex interplay of FBS with other nonlinearities and often result in cascaded dynamics. Extreme examples of this are lasers that are passively mode-locked at the acoustic resonance frequency [36, 37]. It should be stressed that in the case of a straight dispersionless waveguide and for strict intra-mode scattering the intensity variations at the end of a waveguide do not differ from those at the front, because the beat of the pump and Stokes lines and among the Stokes lines vanishes exactly. This is the reason why many measurements are either done in orthogonal polarizations or in interferometric setups that are designed to eliminate the main pump line [6–11]. Through the amplitude and phase modifications of the individual Stokes order this leads to a beat signal, which can then be easily detected by a photodiode and analyzed in the RF domain. It should be noted that the relative amplitudes of the lines in the RF spectrum can differ considerably from relative amplitudes in the actual optical spectrum.

In contrast, experiments on FBS in integrated photonics often require a pump-probe configuration with fairly strong Stokes seeds in order to lift the spectral peaks above the detection threshold. As a consequence, the measurements are usually not sensitive enough to distinguish between 'stimulated' (in the sense of 'self-amplifying') dynamics and an 'optically driven' phase modulation. Furthermore, these experiments may not require special 'phase-mixing' elements (e.g. interferometric loops) to convert the pure phase modulation into a partial intensity modulation, because (narrow-band) grating couplers readily introduce phases and the waveguides are dispersive in themselves. Quite often, the interaction lengths are too short for cascading to set in. Without the need to capture cascading, the theoretical description is often restricted to basic coupled-mode theory borrowed from backward SBS. Only recently, an extension of the coupled-mode formulation to include the first anti-Stokes line has led to the realization [18] that self-amplifying FBS is not generally expected in integrated waveguides. Care should be taken when studying FBS in weakly dispersive integrated waveguides with broad-band couplers (or even butt-coupling): without the phase modification to the individual Stokes orders, this will only result in a pure phase modulation that will go un-noticed if directly analyzed with a photo diode.

6.3. Stimulated versus Raman-like scattering

As we have mentioned in the introduction, FBS is known under different names, especially as 'Raman-like' or as 'forward stimulated' scattering. Each of them is justified, because they indicate features that may or may not be dominant depending on the specific type of waveguide and the measurement technique employed. For example, in section 5.2, we have clearly shown that intra-mode FBS is phenomenologically indistinguishable from a low-frequency tail of the Raman spectrum if and only if the acoustic group velocity (i.e. the velocity at which an acoustic pulse travels along the waveguide) is negligibly small. This is usually the case in intra-mode FBS and inter-mode FBS between degenerate optical modes (see figure 8). In these systems the term 'Raman-like' is well justified. Large acoustic group velocities can occur for inter-mode FBS or if the acoustic dispersion relation has a Dirac point at $q = 0$. The formation of Dirac points through the combination of symmetry-related and accidental degeneracies at the Γ-point is well understood in the context of photonic crystals [38] and similar

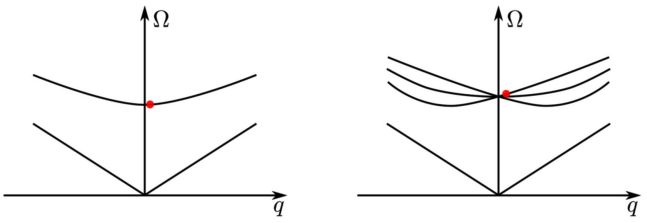

Figure 8. Schematic examples for acoustic dispersion relations with low acoustic group velocity of the higher-order acoustic mode (red dot in left panel) and with a Dirac point at $q = 0$ leading to high acoustic group velocities of some of the higher-order acoustic modes (red dot in right panel). FBS in the conventional case with low acoustic group velocity can be described as a low-frequency contribution to the local Raman response. In contrast, FBS in the right-hand case manifests as a non-local effect along the waveguide. It should be noted that the question whether self-amplification can occur is not related to this, but determined by the *optical* dispersion relation.

effects are expected in mechanical systems, as well. In these two cases, FBS differs from Raman scattering in that it becomes non-local over the length scale of the acoustic decay length (approx. 50–100 μm), which can be very relevant in integrated photonics [39].

Both Brillouin scattering processes, forward and backward, are referred to as SBS in parts of the literature, while some authors restrict this terminology to the backward scattering process, only. The observation that FBS in the absence of dispersion does not result in any amplification of the Stokes signal prompts the question: should FBS be classified as a stimulated process? The answer to this depends on one's definition of what a stimulated process entails. In the context of backward Brillouin scattering and Raman scattering, the term 'stimulated' scattering has been used since the early papers [19, 20] to denote the positive feedback that results in self-amplification of both the optical and acoustic fields. Using this definition a clear distinction is drawn between the spontaneous processes, in which the pump signal is too weak to cause a runaway effect so strong that thermal excitations are amplified to levels comparable to the pump power, and the stimulated process, in which significant self-amplification occurs and the backscattered Stokes signal grows exponentially along the length of the waveguide. This definition applies to FBS provided that the waveguide exhibits an appropriate optical dispersion, as we have shown in section 5, but does not if this condition is not met. Adopting this pragmatic approach, it seems fair to call FBS a stimulated process, but to keep in mind that whether or not the effect is 'stimulated' will always depend on the details of the waveguide and experiment. While the presence of dispersion certainly allows forward amplification, our analysis shows that for the zero dispersion case, or more physically, for distances shorter than the dispersion length, there is no significant self-amplification at powers where amplification would certainly be seen in the backwards case. This suggests that while FSBS is a defensible terminology, perhaps FBS is to be preferred in generality.

6.4. Similarities to cavity opto-mechanics and discrete diffraction

The problem of FBS bears similarities to other fields of optics apart from backward SBS and Raman scattering. One example is the close similarity between FBS in dispersive waveguides and side-band heating and cooling in cavity opto-acoustics [40]. In both cases the opto-acoustic interaction can either suppress acoustic vibrations or lead to an exponential growth. The particular outcome is determined by the imbalance of the optical density of states on the red and the blue side of the optical pump beam. Such a connection is somewhat expected given the intimate connection between both fields [27]. However, there is one fundamental difference: in cavity opto-acoustics, the acoustic oscillations are amplified or suppressed over time, whereas in FBS they are modified along the waveguide.

While cavity opto-acoustics and FBS are clearly based on the same physics, the intimate connection between FBS and discrete diffraction in waveguide arrays is on a formal rather than a physical level. The various Stokes orders constitute channels of light propagation similar to an array of waveguides and a transversal acoustic mode provides a coupling between these channels, whose magnitude is proportional to the acoustic amplitude. It is a fortunate coincidence that in the absence of optical dispersion the acoustic amplitude is constant along the waveguide, i.e. that the process of FBS is formally equivalent to an array of parallel waveguides. As a result, the evolution of the optical intensity through the Stokes orders along the waveguide is governed by the same equations and the solution of the two-tone problem (section 4.2) is identical to the diffraction of light in an array of parallel waveguides. One of the intriguing features of this analogy is that the inter-channel coupling coefficient (or alternatively the effective length ζ of the waveguide array) can be tuned with extreme flexibility via the optical pump power. This similarity raises the possibility for FBS-based quantum-walk experiments.

6.5. Summary and conclusions

We have presented here a new and rigorous formulation of the FBS process, which implicitly includes all coupling amongst the comb of cascaded orders. Because the differences between the quantum and classical formulations are minimal, we have chosen the more general case for our derivation of the equations of motion, beginning with the full optomechanical Hamiltonian of the system. This formalism can therefore be applied to problems of interest in the limit of low photon/phonon numbers, and would be especially useful for the prediction and interpretation of single phonon scattering experiments.

The established description of FSB is derived from the theory of the backward SBS process in fibers. In this, the pump and Stokes fields are modeled as independent, spectrally extremely narrow fields. This is partially motivated by the strong dependence of the acoustic frequency on the optical wave length and the narrow acoustic resonances. Cascading effects can occur in backward SBS [25], but are not a very common feature. Instead, exponential growth of the optical and acoustic amplitudes along the waveguide is the most common manifestation. In contrast, FBS is mostly independent of the optical wavelength, it has a strong tendency towards cascading and requires the help of optical dispersion to have any impact on the optical and acoustic intensities. Thus, the multi-mode ansatz that is so successful in BSBS is not ideal for FBS. We find that a description coupling only one broad-band optical field to an acoustic field is much better suited.

In particular for the dispersionless case we find closed-form solutions, in which the amplitude of the cascaded orders is given simply by a series of Bessel functions. The simplicity of this result follows from one of the main insights arising from this formalism: that the acoustic field exerts, in the absence of dispersion, a pure phase modulation on the optical field. This implies that for dispersionless waveguides FBS is not capable of amplifying the intensity beat between a pump and a Stokes signal.

Acknowledgments

We acknowledge financial support of the Australian Research Council via the ARC Center of Excellence CUDOS (CE110001018) and its Laureate Fellowship (Prof Eggleton, FL120100029) program. Furthermore, we are deeply indebted to Dr Mark Craddock for insightful discussions.

Appendix. Derivation of first-order perturbative dispersion terms

Here we derive the corrections to the optical and acoustic fields for the dispersive dynamics shown in equations (98) and (99).

We start with the dispersion-free stationary two-tone solution:

$$h_0(z,\,t) \approx \log|F_0|, \tag{A1}$$

$$g_0(z,\,t) = \mathrm{i}G_0 \exp\left(-\mathrm{i}\Omega_0 \frac{vt - z}{v}\right), \tag{A2}$$

$$j_0(z,\,t) = \frac{2G_0\omega_0 z}{v} \sin\left(\Omega_0 \frac{vt - z}{v}\right), \tag{A3}$$

with real positive G_0. The correction to p satisfies:

$$\partial_t h_1 + [v + 2w(\partial_z j_0)]\partial_z p = -w\partial_z^2 j_0, \tag{A4}$$

with the boundary condition at $z = 0$

$$h_1(0,\,t) = 0. \tag{A5}$$

The derivatives of the unperturbed phase function are:

$$\partial_z j_0 = \frac{G_0\omega_0}{v} \sin\left(\Omega_0 \frac{vt - z}{v}\right) - \frac{G_0\omega_0\Omega_0 z}{v^2} \cos\left(\Omega_0 \frac{vt - z}{v}\right), \tag{A6}$$

$$\partial_z^2 j_0 = -\frac{4G_0\omega_0\Omega_0}{v^2} \cos\left(\Omega_0 \frac{vt - z}{v}\right) - \frac{2G_0\omega_0\Omega_0^2 z}{v^3} \sin\left(\Omega_0 \frac{vt - z}{v}\right). \tag{A7}$$

The dispersive correction to the effective group velocity is of order w and therefore introduces corrections of order w. We may therefore approximate:

$$(\partial_t + v\partial_z)h_1 = \frac{2w\omega_0\Omega_0 G_0}{v^3}\left[2v \cos\left(\Omega_0 \frac{vt - z}{v}\right) + \Omega_0 z \sin\left(\Omega_0 \frac{vt - z}{v}\right)\right]. \tag{A8}$$

Through the substitution

$$y = vt + z, \qquad s = t - \frac{z}{v}; \tag{A9}$$

$$z = \frac{y - vs}{2}, \qquad t = \frac{y + vs}{2v}, \tag{A10}$$

this can be reduced to the ordinary differential equation

$$v\partial_y = \frac{2w\omega_0\Omega_0 G_0}{v^3}\left[2v\cos\Omega_0 s + \frac{\Omega_0(y - vs)}{2}\sin\Omega_0 s\right]. \tag{A11}$$

With the explicit solution:

$$h_1(y, s) = \frac{w\omega_0\Omega_0 G_0}{v^4}\int_0^y \mathrm{d}y'\left[2v\cos(\Omega_0 s) + \Omega_0\frac{y' - vs}{2}\sin(\Omega_0 s)\right] + C(s), \tag{A12}$$

$$= \frac{w\omega_0\Omega_0 G_0}{v^4}\left[2vy\cos(\Omega_0 s) + \frac{\Omega_0}{4}(y^2 - 2yvs)\sin(\Omega_0 s)\right] + C(s), \tag{A13}$$

where $C(s)$ is defined through the boundary condition expressed in the transformed coordinates $h_1(vs, s) = 0$. Therefore, the first order correction to p is:

$$h_1(y, s) = \frac{w\omega_0\Omega_0 G_0}{v^4}\left[2v(y - vs)\cos(\Omega_0 s) + \frac{\Omega_0}{4}(y - vs)^2\sin(\Omega_0 s)\right]; \tag{A14}$$

$$h_1(z, t) = \frac{w\omega_0\Omega_0 G_0}{v^4}\left[4vz\cos\left(\Omega_0\frac{vt - z}{v}\right) + \Omega_0 z^2\sin\left(\Omega_0\frac{vt - z}{v}\right)\right]. \tag{A15}$$

This recovers equation (98) in the main text.

The remaining step is to find the correction to the acoustic problem:

$$g_0(z, t) + g_1(z, t) = \mathrm{i}\Omega_0\int_0^\infty \mathrm{d}t'\,\mathrm{e}^{-\gamma t' - \mathrm{i}\Omega_0 t'}\,|A(t - t' - z/v)|^2\exp[2h_1(z, t - t')] \tag{A16}$$

$$\approx \mathrm{i}\Omega_0\int_0^\infty \mathrm{d}t'\,\mathrm{e}^{-\gamma t' - \mathrm{i}\Omega_0 t'}\,|A(t - t' - z/v)|^2[1 + 2h_1(z, t - t')] \tag{A17}$$

$$= g_0(z, t) + \underbrace{2\Omega_0\mathrm{i}\int_0^\infty \mathrm{d}t'\,\mathrm{e}^{-\gamma t' - \mathrm{i}\Omega_0 t'}\,|A(t - t' - z/v)|^2 h_1(z, t - t')}_{=g_1(z,t)}. \tag{A18}$$

Assuming that the intensity of the incident optical signal varies only weakly (weak incident Stokes seed, e.g. due to thermal fluctuations), we can replace $|F(t)|^2 \approx |F_0|^2$ in the second term:

$$g_1(z, t) \approx \frac{2\mathrm{i}w\omega_0\Omega_0^2 G_0|F_0|^2}{v^4}\int_0^\infty \mathrm{d}t'\,\mathrm{e}^{-\gamma t' - \mathrm{i}\Omega_0 t'}\left[4vz\cos\left(\Omega_0\frac{vt - vt' - z}{v}\right) + \Omega_0 z^2\sin\left(\Omega_0\frac{vt - vt' - z}{v}\right)\right] \tag{A19}$$

$$\approx \frac{2\mathrm{i}w\omega_0\Omega_0^2 G_0|F_0|^2}{v^4\gamma}[4vz + \mathrm{i}\Omega_0 z^2]\exp\left(\mathrm{i}\Omega_0\frac{z - vt}{v}\right), \tag{A20}$$

where only retained the resonant contribution to the convolution. This is the second expression required in the main text.

References

[1] Brillouin L 1922 Diffusion de la lumière par un corps transparent homogène *Ann. Phys., Paris* **17** 88–122

[2] Boyd R W 2008 *Nonlinear Optics* 3rd edn (New York: Academic)

[3] Agrawal G P 2012 *Nonlinear Fiber Optics* 5th edn (New York: Academic) p 529

[4] Eggleton B J, Poulton C G and Pant R 2013 Inducing and harnessing stimulated Brillouin scattering in photonic integrated circuits *Adv. Opt. Photonics* **5** 536–87

[5] Shelby R M, Levenson M D and Bayer P W 1985 Guided acoustic-wave Brillouin scattering *Phys. Rev.* B **31** 5244–52

[6] Elser D, Andersen U L, Korn A, Glöckl O, Lorenz S, Marquardt Ch and Leuchs G 2006 Reduction of guided acoustic wave Brillouin scattering in photonic crystal fibers *Phys. Rev. Lett.* **97** 133901

[7] Dainese P, Russell P St J, Wiederhecker G S, Joly N, Fragnito H L, Laude V and Khelif A 2006 Raman-like light scattering from acoustic phonons in photonic crystal fiber *Opt. Express* **14** 4141–50

[8] Beugnot J-C, Sylvestre T, Maillotte H, Mélin G and Laude V 2007 Guided acoustic wave Brillouin scattering in photonic crystal fibers *Opt. Lett.* **32** 17–9

[9] Kang M S, Brenn A, Wiederhecker G S and Russell P St J 2008 Optical excitation and characterization of gigahertz acoustic resonances in optical fiber tapers *Appl. Phys. Lett.* **93** 131110

[10] Stiller B, Delqué M, Beugnot J-C, Lee M W, Mélin G, Maillotte H, Laude V and Sylvestre T 2011 Frequency-selective excitation of guided acoustic modes in a photonic crystal fiber *Opt. Express* **19** 7689–94

[11] nee Zhong W E, Stiller B, Elser D, Heim B, Marquardt C and Leuchs G 2015 Depolarized guided acoustic wave Brillouin scattering in photonic crystal fibers *Opt. Express* **23** 27707–14
[12] Renninger W H, Shin H, Behunin R O, Kharel P, Kittlaus E A and Rakich P T 2016 Forward Brillouin scattering in hollow-core photonic bandgap fibers *New J. Phys.* **18** 025008
[13] Shin H, Qiu W, Jarecki R, Cox J A, Olsson R H, Starbuck A, Wang Z and Rakich P T 2013 Tailorable stimulated Brillouin scattering in nanoscale silicon waveguides *Nat. Commun.* **4** 1944
[14] Van Laer R, Bazin A, Kuyken B, Baets R and Thourhout D V 2015 Net on-chip Brillouin gain based on suspended silicon nanowires *New J. Phys.* **17** 115005
[15] Van Laer R, Kuyken B, Van Thourhout D and Baets R 2014 Analysis of enhanced stimulated Brillouin scattering in silicon slot waveguides *Opt. Lett.* **39** 1242–5
[16] Chen G, Zhang R, Sun J, Xie H, Gao Y, Feng D and Xiong H 2014 Mode conversion based on forward stimulated Brillouin scattering in a hybrid phononic-photonic waveguide *Opt. Express* **22** 32060–70
[17] Van Laer R, Kuyken B, Van Thourhout D and Baets R 2015 Interaction between light and highly confined hypersound in a silicon photonic nanowire *Nat. Photon.* **9** 199–203
[18] Kharel P, Behunin R O, Renninger W H and Rakich P T 2016 Noise and dynamics in forward Brillouin interactions *Phys. Rev.* A **93** 063806
[19] Shen Y R and Bloembergen N 1965 Theory of stimulated Brillouin and Raman scattering *Phys. Rev.* **137** 1787–805
[20] Tang C L 1966 Saturation and spectral characteristics of the Stokes emission in the stimulated Brillouin process *J. Appl. Phys.* **37** 2945–55
[21] Lee H, Hayashi N, Mizuno Y and Nakamura K 2016 Slope-assisted Brillouin optical correlation-domain reflectometry: proof of concept *IEEE Photonics J.* **8** 1–7
[22] Bongrand I, Picozzi A and Picholle E 1998 Coherent model of cladding Brillouin scattering in singlemode fibres *Electron. Lett.* **34** 1769–70
[23] Rakich P T, Reinke C, Camacho R, Davids P and Wang Z 2012 Giant enhancement of stimulated Brillouin scattering in the subwavelength limit *Phys. Rev.* X **2** 011008
[24] Wolff C, Steel M J, Eggleton B J and Poulton C G 2015 Stimulated Brillouin scattering in integrated photonic waveguides: forces, scattering mechanisms and coupled mode analysis *Phys. Rev.* A **92** 013836
[25] Büttner T F S, Kabakova I V, Hudson D D, Pant R, Poulton C G, Judge A C and Eggleton B J 2014 Phase-locking and pulse generation in multi-frequency Brillouin oscillator via four wave mixing *Sci. Rep.* **4** 5032
[26] Büttner T F S, Merklein M, Kabakova I V, Hudson D D, Choi D-Y, Luther-Davies B, Madden S J and Eggleton B J 2014 Phase-locked, chip-based, cascaded stimulated Brillouin scattering *Optica* **1** 311–4
[27] Van Laer R, Baets R and Van Thourhout D 2016 Unifying Brillouin scattering and cavity optomechanics *Phys. Rev.* A **93** 053828
[28] Kang M S, Nazarkin A, Brenn A and Russell P St J 2009 Tightly trapped acoustic phonons in photonic crystal fibres as highly nonlinear artificial Raman oscillators *Nat. Phys.* **5** 276–80
[29] Sipe J E and Steel M J 2016 A Hamiltonian treatment of stimulated Brillouin scattering in nanoscale integrated waveguides *New J. Phys.* **18** 045004
[30] Gordon J P 1986 Theory of the soliton self-frequency shift *Opt. Lett.* **11** 662–4
[31] Montes C and Pellat R 1987 Inertial response to nonstationary stimulated Brillouin backscattering: damage of optical and plasma fibers *Phys. Rev.* A **36** 2976–9
[32] Rakich P T and Marquardt F 2016 Quantum theory of continuum optomechanics arXiv:1610.03012
[33] Kittlaus E A, Shin H and Rakich P T 2016 Large Brillouin amplification in silicon *Nat. Photon.* **10** 463
[34] Wolff C, Gutsche P, Steel M J, Eggleton B J and Poulton C G 2015 Impact of nonlinear loss on stimulated Brillouin scattering *J. Opt. Soc. Am.* B **32** 1968
[35] Dong M and Winful H G 2016 Unified approach to cascaded stimulated Brillouin scattering and frequency-comb generation *Phys. Rev.* A **93** 043851
[36] Kang M S, Joly N Y and Russell P St J 2013 Passive mode-locking of fiber ring laser at the 337th harmonic using gigahertz acoustic core resonances *Opt. Lett.* **38** 561–3
[37] Stiller B and Sylvestre T 2013 Observation of acoustically induced modulation instability in a Brillouin photonic crystal fiber laser *Opt. Lett.* **38** 1570–2
[38] Huang X, Lai Y, Hang Z H, Zheng H and Chan C T 2011 Dirac cones induced by accidental degeneracy in photonic crystals and zero-refractive-index materials *Nat. Mater.* **10** 582–6
[39] Wolff C, Steel M J, Eggleton B J and Poulton C G 2015 Acoustic build-up in on-chip stimulated Brillouin scattering *Sci. Rep.* **5** 13656
[40] Bahl G, Tomes M, Marquardt F and Carmon T 2012 Observation of spontaneous Brillouin cooling *Nat. Phys.* **8** 203–7